2012

Reconfigurable Wideband Circulalry Polarized Microstrip Antenna for Wireless Applications

Ahmed Khidre

Reconfigurable Wideband Circularly Polarized Microstrip Patch Antenna for Wireless Applications

A Thesis

Presented in partial fulfillment of the requirements for

Master of Science

Degree

Electrical Engineering

The University of Mississippi

Ahmed Khidre

May 2012

ABSTRACT

In this thesis, developments of rectangular microstrip patch antenna to have circular polarization agility with wideband performance, for wireless applications are presented. First, a new technique to achieve circularly polarized (CP) probe feed single-layer microstrip patch antenna with wideband characteristics is proposed. The antenna is a modified form of the popular E-shaped patch, used to broaden the impedance bandwidth of a basic rectangular patch antenna. This is established by letting the two parallel slots of the E-patch unequal. Thus, by introducing asymmetry two orthogonal currents on the patch are excited and circularly polarized fields are realized. The proposed technique exhibits the advantage of the simplicity inherent in the E-shaped patch design. It requires only slot lengths, widths, and position parameters to be determined. Also, it is suitable for later adding the reconfigurable capability. With the aid of full-wave simulator Ansoft HFSS, investigations on the effect of various dimensions of the antenna have been carried out via parametric analysis. Based on these investigations, a design procedure for a CP E-shaped patch is summarized. Various design examples with different substrate thicknesses and material types are presented and compared, with CP U-slot patch antennas, recently proposed in the literature. A prototype has been constructed following the suggested design procedure to cover the *IEEE 802.11b/g* WLAN band. The performance of the fabricated antenna was measured and compared with the simulation results for the reflection coefficient, axial ratio, radiation pattern, and antenna gain. Good agreement is achieved between simulation and measured results demonstrating a high gain and wideband performance.

Second**,** a polarization reconfigurable single feed E-shaped patch antenna with wideband performance is proposed. The antenna is capable of switching from right-hand circular polarization (RHCP) to left-hand circular polarization (LHCP) and vice versa, with the aid of two RF PIN diodes that act as RF switches. The proposed structure which is simple; consists of a single-layer single fed radiating E-shaped patch and RF switch placed on each of its slots at an appropriate location. The design targets WLAN *IEEE 802.11b/g* frequency band (2.4-2.5 GHz) as one example of the wireless applications. The idea is based on the first proposed design. In other words, if one of the switches is ON and the other is OFF, the two slot lengths will become effectively unequal and circular polarization will be obtained. If the states of the two switches are reversed, circular polarization with opposite orientation will be obtained at the same frequency band. Full-wave simulator Ansoft HFSS is again used for the analysis. Complete detailed DC biasing circuit of the switches for integration with the antenna is presented. Also, characterizations of the microwave components used in the biasing circuit are discussed. Antenna prototype has been fabricated and tested. Simulation results along with the measured one, for the reflection coefficient, axial ratio, radiation pattern, and antenna gain agree well, showing wide bandwidth and high gain for the two circularly polarized modes.

DEDICATIONS

To my mom, dad, brothers, uncles, and cousins

for their love, motivation, prayers and bless

LIST OF ABBREVIATIONS

AR	Axial Ratio
BW	Bandwidth
AC	Alternating Current
CP	Circularly Polarized
DC	Direct Current
GPS	Global Positioning System
HFSS	High Frequency Structure Simulation
LHCP	Left-Hand Circular Polarization
MIMO	Multiple Input Multiple Output
RHCP	Right-Hand Circular Polarization
RFID	Radio Frequency Identification
RF	Radio Frequency
PCB	Printed Circuit Board
WLAN	Wireless Local Area Network

ACKNOWLEDGMENTS

This is to acknowledge professor Kai-Fong Lee for his guiding ideas, and fruitful discussions during the work on this thesis. Also, I'm grateful to my advisors professor Atef Elsherbeni and professor Fan Yang for their helpful discussion, teaching me, and being patient while reading and correcting my thesis.

I'd like also to thank Mr. Marty Hickman, the laboratories supervisor at the electrical engineering department, for helping me in building up the antenna prototypes for measurements.

TABLE OF CONTENT

ABSTRACT ..... **I**

DEDICATIONS ..... **III**

LIST OF ABBREVIATIONS ..... **IV**

ACKNOWLEDGMENTS ..... **V**

LIST OF TABLES ..... **VIII**

LIST OF FIGURES ..... **IX**

INTRODUCTION **1**

1.1 Circular Polarization Scheme 1

1.2 Circularly Polarized Microstrip Antennas 2

1.3 Polarization Reconfigurable Microstrip Antennas 3

1.4 Organization of the Thesis 4

BACKGROUND **6**

2.1 Wideband Circularly Polarized Microstrip Antennas 6

2.2 Polarization Reconfigurable Microstrip Antennas 8

2.3 RF Switching 10

2.4 Motivations 13

CP E-SHAPED MICROSTRIP PATCH ANTENNA **15**

3.1 Antenna Geometry and CP Mechanism 15

3.1.1 Antenna Configuration *15*

3.1.2 The CP Design *15*

3.2 Parametric Analysis and Design Procedure 19

3.2.1 Parametric Study *19*

3.2.2 Design Procedure *23*

3.3 Design Examples and Comparison with CP U-Slot Antenna 24

3.3.1 Design I *25*

3.3.1 Design II *29*

3.4 Fabrication and Measurements of CP E-Shaped Patch Antenna 30

RECONFIGURABLE E-SHAPED PATCH ANTENNA 35

4.1 Principle of Operation 35

4.2 Antenna Geometry 36

4.3 Biasing Circuitry and Simulation Results 39

4.4.1 DC Block Capacitors *39*

4.4.2 RF PIN Diode Switch *39*

4.4.3 Simulation Results *43*

4.4 Antenna Prototype and Experimental Verification 44

CONCLUSION AND FUTURE WORK 49

5.1 Contributions 49

5.2 Future Work 50

BIBLIOGRAPHY 51

LIST OF PUBLICATIONS 56

VITA 57

LIST OF TABLES

Table 2.1 Antenna switching states [16]..... 11

Table 2.2 Antenna switching states Table 2.2 [26]. 13

Table 3.1 Dimensions of linear polarized E-shaped patch in mm 16

Table 3.2 Dimensions of CP E-shaped patch in mm 27

Table 3.3 Dimensions of CP unequal U-slot patch in mm 28

Table 3.4 Dimensions of CP truncated corner U-slot patch in mm 28

Table 3.5 Dimensions of CP E-shaped patch prototype in mm 31

Table 4.1 Antenna possible configurations 36

Table 4.2 Antenna bandwidth simulated vs. measured results at states 3, 4 47

LIST OF FIGURES

Figure 1.1 Illustration for a right-hand circularly polarized electromagnetic wave [1]. 2

Figure 1.2 Commercial CP microstrip antennas. (a) Amotech ceramic patches for GPS [2]. (b) Manufactured by ETS-Lindgren. 2

Figure 1.3 Polarization reconfigurable antennas. (a) Linear polarization agility. (b) Circular polarization agility. 4

Figure 2.1 Illustration for the different methods to achieve CP from a patch antenna. (a) Sequential rotation array [5] . (b) Tab to an elliptical patch [6]. (c) Truncated corners [7]. (d) 45° narrow slot [8]. 7

Figure 2.2 Broadband microstrip antennas. (a) U-slot [11]. (b) E-shaped [14]. 7

Figure 2.3 Broadband CP U-slot microstrip antenna (a) Geometry of CP unequal arms U-slot antenna [17]. (b) Geometry of CP truncated corners U-slot antenna [18]. 8

Figure 2.4 Reconfigurable microstrip antenna for switchable polarization [19]. 11

Figure 2.5 Reconfigurable microstrip antenna with switchable polarization [20]. 11

Figure 2.6 Reconfigurable U-slot antenna [24]. 12

Figure 2.7 Reconfigurable circular patch with switchable polarization [25]. 12

Figure 2.8 Reconfigurable microstrip antenna with quadruple switched polarization [26]. 12

Figure 2.9 Different packages of RF PIN diode manufactured by Skyworks [28]. 13

Figure 2.10 RF MEMs switch by the Laboratory for Analysis and Architecture of Systems: LAAS-CNRS [30] 13

Figure 3.1 Antenna geometry. 16

Figure 3.2 Current flow across patch. (a) Linear polarized E-patch. (b) Circular polarized E-shaped patch. 16

Figure 3.3 Current vector distribution on the CP E-shaped patch and zoomed part of it at different phase state. 18

Figure 3.4 Current vector distribution on the CP E-shaped patch and zoomed part of it at different phase state. 19

Figure 3.5 S_{11} at different values of Ls1 while the other parameters in Table 3.1 are fixed. 20

Figure 3.6 Axial ratio at different values of Ls1 while the other parameters in Table 3.1 are fixed. 21

Figure 3.7 S_{11} at different values of F and Ls1=17 mm while the other parameters in Table 3.1 are fixed. 22

Figure 3.8 Axial ratio at different values of F1 and Ls1=17 mm while the other parameters in Table 3.1 are fixed. 22

Figure 3.9 S_{11} at different values of Ls2 while Ls1=17 mm, F=16 mm, and other parameters in Table 3.1 are fixed. 23

Figure 3.10 Axial ratio at different values of Ls2 while Ls1=17 mm, F=16 mm, and other parameters in Table 3.1 are fixed. 24

Figure 3.11 Flow chart for the design and tuning procedure. 26

Figure 3.12 Geometry of CP unequal arms U-slot antenna [17]. 27

Figure 3.13 Geometry of CP truncated corners U-slot antenna [18]. 27

Figure 3.14 S_{11} for E-shaped, unequal arms U-slot, and truncated corners U-slot antennas. 28

Figure 3.15 Axial ratio for E-shaped, unequal arms U-slot, and truncated corners U-slot antennas. 28

Figure 3.16 S_{11} for E-shaped, unequal arms U-slot, and truncated corners U-slot antennas. 29

Figure 3.17 Axial ratio for E-shaped, unequal arms U-slot, and truncated corners U-slot antennas. 30

Figure 3.18 Prototype of CP E-shaped patch antenna (a) plane view, (b) side view. 31

Figure 3.19 Simulation vs. measurements of S_{11} for CP E-shaped patch antenna. 32

Figure 3.20 Simulation vs. measurements of axial ratio for CP E-shaped patch antenna. 33

Figure 3.21 Radiation pattern of circular fields at 2.45GHz (a) yz (b) xz. 33

Figure 3.22 Simulation vs. measured broadside gain versus frequency. 34

Figure 4.1 Switching states of the E-shaped patch antenna (a) state 1 (b) state 2 (c) state 3 (d) state 4. 36

Figure 4.2 Current distribution on E-shaped patch antenna in state 3. 36

Figure 4.3 Geometry of a single feed reconfigurable E-shaped patch antenna with integrated DC biasing circuit. (a) Top view. (b) Side view. L_{sub} =140mm, W_{sub} =80mm, L=43mm, W=77mm, L_s=30mm, W_s=7mm, Y_f =14mm, P=17mm, L_{st} =28mm, W_{st} = 0.3mm, S=0.5mm, h=10mm, t=0.787mm. 38

Figure 4.4 A 50Ω microstrip line with a narrow slit of 0.5 mm at the middle of it for characterizing the DC block capacitors and RF PIN diode switch.....39

Figure 4.5 Magnified picture of the capacitor ATC600F100, mounted over 50Ω transmission line. 40

Figure 4.6 Measured S-parameters of the capacitor ATC600F100 mounted over a 50Ω transmission line. 40

Figure 4.7 The linear circuit model of the PIN diode (MA4SPS402) in both ON/OFF states used in simulation at I_f =10mA. 41

Figure 4.8 Setup for PIN diode insertion and return loss measurements.....42

Figure 4.9 Magnified picture of PIN diode (MA4SPS402) mounted over 50Ω microstrip line for characterization. 42

Figure 4.10 Insertion loss for the MA4SPS402 PIN diode, at I_f=10mA, V_f =0.94 V using 50 transmission line setup. 42

Figure 4.11 Power transfer relation of MA4SPS402 PIN diode using 50Ω transmission line setup. 43

Figure 4.12 Simulation results for S11 of the reconfigurable E-shaped patch antenna in state 3 at different diodes' locations. 44

Figure 4.13 Simulation results for axial ratio of the reconfigurable E-shaped patch antenna in state 3 at different diodes locations.....44

Figure 4.15 Simulated and measured S_{11} for the proposed antenna in states 3, 4. 46

Figure 4.16 Simulated and measured axial ratio for the proposed antenna in states 3, 4. 47

Figure 4.17 Simulated and measured radiation pattern of the proposed antenna. (a) x-z plane at state 3. (b) y-z plane at state 3. (c) x-z plane at state 4 (d) y-z plane at state 4.....48

Figure 4.18 Simulate and measure gain of the proposed antenna in either states 3 or state 4. 48

CHAPTER 1

INTRODUCTION

1.1 Circular Polarization Scheme

Circularly polarized waves consist of two perpendicular electromagnetic plane waves of equal amplitude and 90° phase difference. Figure 1.1 illustrates right-hand circular polarization (RHCP). If the wave is composed of two plane waves of equal amplitude and differing in phase by 90°, it is said to be circularly polarized where the tip of the electric field vector appears to be moving in a circle. Looking at the wave source, if the electric field vector of the wave coming toward you appears to be rotating counterclockwise, the wave is said to be right-circularly polarized. Whereas, it is clockwise, the wave is said to be left-circularly polarized light. The electric field vector makes one complete revolution as the wave advances one wavelength toward you. Another way of demonstrating; if the thumb of your right hand were pointing in the direction of propagation of the light, the electric vector would be rotating in the direction of your fingers.

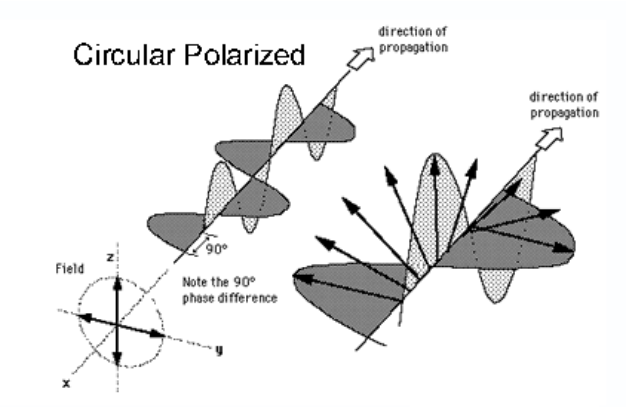

Figure 1.1 Illustration for a right-hand circularly polarized electromagnetic wave [1].

1.2 Circularly Polarized Microstrip Antennas

Circularly polarized microstrip antennas are attractive for wireless applications, because they combine the advantages of both circular polarization characteristics and microstrip antennas. A circularly polarized wave radiates energy in the horizontal, vertical planes as well as every plane in between. Thus, circular polarization can reduce the transmission loss caused by the polarization misalignment between antennas of stationary and mobile terminals. Moreover, it gives a higher probability of a successful link, better mobility, weather penetration, and system performance enhancement relative to linear polarization. On the other hand, microstrip antennas have planar profile, low cost, and mechanical robustness. CP microstrip antennas have been widely used in different current wireless applications such as GPS and RFID reader systems. Examples of a commercial CP microstrip patch antenna are shown in Figure 1.2.

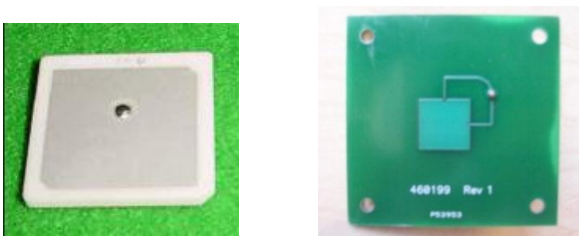

(a) (b)

Figure 1.2 Commercial CP microstrip antennas. (a) Amotech ceramic patches for GPS [2]. (b) Manufactured by ETS-Lindgren.

1.3 Polarization Reconfigurable Microstrip Antennas

Polarization reconfigurable microstrip antennas have received much attention in the last decade. They are sometimes called “polarization agile microstrip antennas” because they can alter their polarization characteristic. Some of them can change from vertical to horizontal polarization and vice versa. These are called “linear polarization agile antennas”. Whereas, others can switch between RHCP and LHCP and vice versa, these are called “circular polarization agile antennas”. Figure 1.3 illustrates the difference between the two types. Also, there are some types of polarization agile antennas that can mix between linear and circular polarization modes.

Polarization reconfigurable microstrip antennas are desired for wireless applications, because they permit doubling the system capacity through frequency reuse with two different polarizations. In addition, they can consent polarization diversity in radio links, which combats signal fading and avoids error bursts. Moreover, they allow users to roam on different wireless systems within the antennas’ bandwidths without the need of several individual antennas integrated in their devices. Hence, they are useful for the compactness and weight reduction of the wireless devices. Furthermore, reconfigurable circularly polarized antennas provide powerful modulation scheme for microwave tagging systems [3]. Recently, polarization reconfigurable antennas prove to have potential applications in multiple-input multiple-output (MIMO) systems [4].

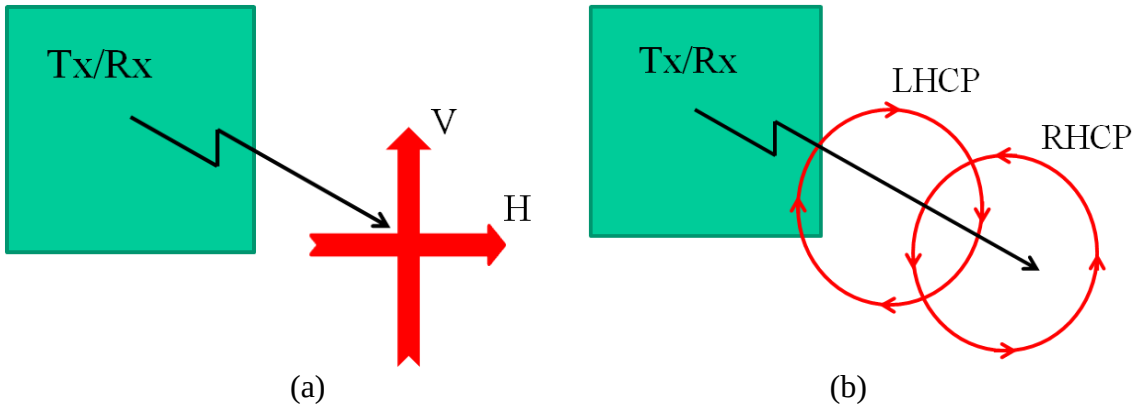

Figure 1.3 Polarization reconfigurable antennas. (a) Linear polarization agility. (b) Circular polarization agility.

1.4 Organization of the Thesis

Chapter 2 presents a background about the various methods to establish CP radiation fields from microstrip antennas with wideband characteristic. In addition, it defines polarization agile antennas and shows methods for reconfiguration. Former efforts, which exist in the literature to acquire wideband CP, as well as polarization reconfigurable microstrip antennas, are also presented. Then, objective and motivation of the thesis work is declared. Chapter 3 discusses the proposed wideband CP E-shaped patch antenna design. In particular, the operation principle, design idea, and design procedure are explained and summarized. Also, various design examples following the suggested procedure are demonstrated, and finally performance measurement for a constructed prototype exists. Chapter 4 presents the operational principle of a reconfigurable E-shaped patch antenna. It explains the antenna geometry with the integrated DC biasing circuit for the PIN diodes switches, including its operation mechanism. In addition to that, it shows the characteristic measurements for the microwave components (PIN diode, microwave capacitor) used in the biasing circuit, and their equivalent circuit model plugged in the full-wave simulation. Furthermore, performance of an antenna prototype at both of its CP modes is addressed in

details. Finally, Chapter 5 presents the contributions of the thesis and suggestions for future work.

CHAPTER 2

BACKGROUND

2.1 Wideband Circularly Polarized Microstrip Antennas

Many studies and research efforts have been reported in the literature to obtain circularly polarized microstrip antenna. They could be classified according to the number of feeds and number of layers. In general, single-feed single-layer structures yield the smallest axial ratio bandwidth (ARBW). However, these structures are attractive because of their simplicity. They do not need external circuitry or larger space compared to the structures of other methods such as dual/multiple-feed/layer and sequential arrays [5]. Techniques used to obtain CP in single-feed single-layer microstrip antennas include trimming opposite corners or cutting a narrow slot at 45° of a square patch, or adding tabs to an elliptical patch [6]. Figure 2.1 illustrates these methods for obtaining CP from patch antennas. However, the obtained ARBW using these techniques is usually less than 1% which limits their practical applications.

For the case of linear polarization, a number of impedance broadening techniques have been developed in the last two decades. In particular, the U-slot [9]-[10], L-probe [12]-[13], and E-shaped microstrip patches [14], who have gained a lot of popularity because they

do not require complex matching network or stacked configuration compared to other methods. Figure 2.2 shows pictures for some of these techniques. More recently, in the last four years, the U-slot and L-probe techniques have been applied to single-layer single-feed CP patch antennas [15]-[18]. These techniques enable the use of thick substrates, and as large as 13% ARBW was obtained. In [18], asymmetric U-slot was incorporated on the patch's surface to perturbs the fields beneath the patch and yield CP. Geometry for this configuration is shown in Figure 2.3a. In [17], the trimmed corner technique for acquiring CP is combined with the U-slot technique for broadening the impedance bandwidth as shown in Figure 2.3a.

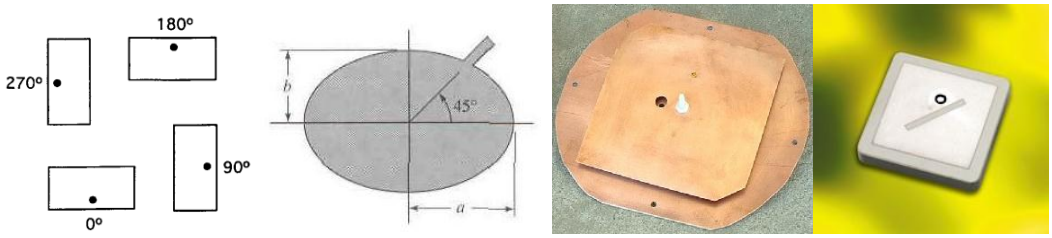

(a) (b) (c) (d)

Figure 2.1 Illustration for the different methods to achieve CP from a patch antenna. (a) Sequential rotation array [5] . (b) Tab to an elliptical patch [6]. (c) Truncated corners [7]. (d) 45° narrow slot [8].

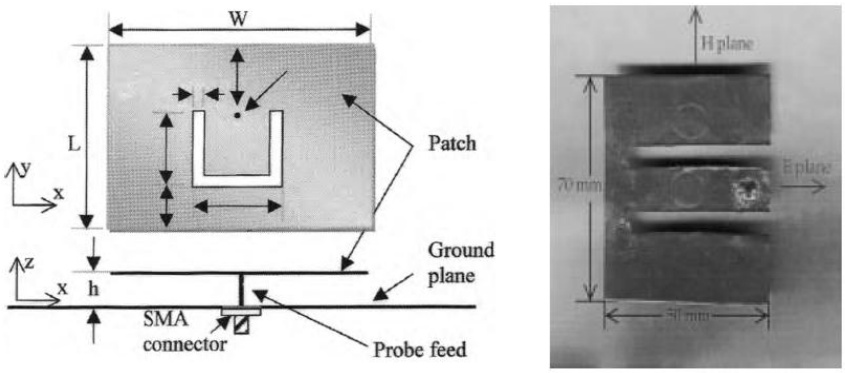

(a) (b)

Figure 2.2 Broadband microstrip antennas. (a) U-slot [11]. (b) E-shaped [14].

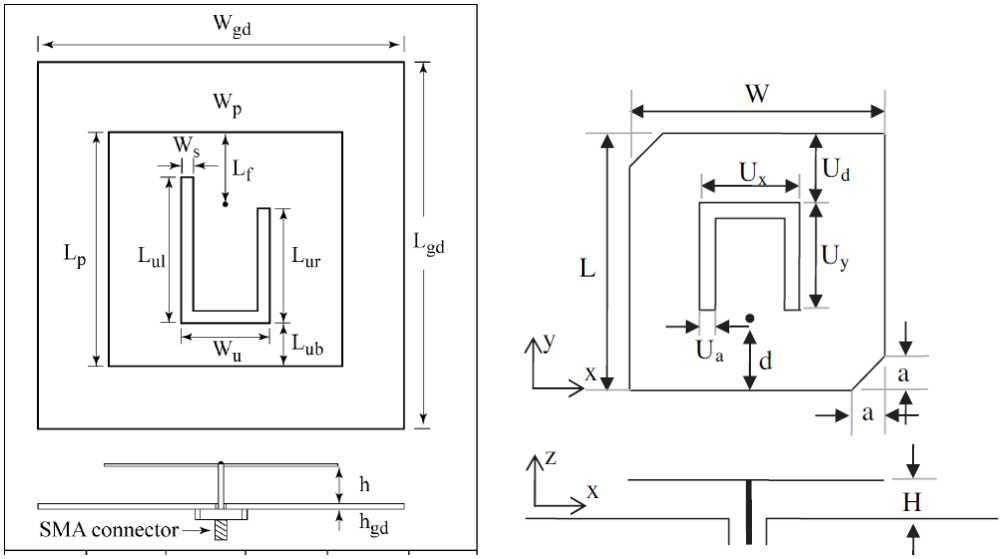

Figure 2.3 Broadband CP U-slot microstrip antenna (a) Geometry of CP unequal arms U-slot antenna [17]. (b) Geometry of CP truncated corners U-slot antenna [18].

2.2 Polarization Reconfigurable Microstrip Antennas

In the literature, many designs with different methods and techniques were reported for polarization agility, such as in [19]-[26]. Antenna proposed in [19] is shown in Figure 2.4. It consists of square patch with two orthogonal slots. Each slot has a switch on the middle of it. Switches are modeled as a metallic pad for proving the concept of switching for reconfigurability. When the upper switch is ON and the other is OFF (state1), RHCP is realized. Whereas, for the reversed case (state 2), LHCP is realized. Antenna bandwidth in both of these states is 3%.

Figure 2.5 shows the antenna proposed in [20]. Basically it is a trimmed corner square patch antenna, with four triangular trimmed parts at the corners. They are allowed to be connected or disconnected via RF switches to the patch. Again, switches are ideally modeled as metallic pads for proving the concept of switching for reconfigurability. Antenna has four switching states tabulated in Table 2.1. It can switch from LP to both RHCP and

LHCP with slight change in resonant frequency. The antenna bandwidth does not exceed 2.6% in CP modes, and its maximum gain is 5.3dBi.

In [24] simple design was proposed, which is based on the unequal arms U-slot CP microstrip antenna. The geometry is shown in Figure 2.6, where a conventional U-slot microstrip antenna is loaded with two switches on each of its arms. When the right switch is ON and the left one is OFF, the U-slot will be equivalently, of unequal arms, hence giving LHCP. Reversing the switching states would give RHCP. Also, if both switches are ON or OFF LP polarization will be obtained. Switching is realized via RF PIN diodes. The proposed design has 2.75% bandwidth in the CP modes with 7.5dBi maximum gain.

In a similar fashion, another design was proposed in [25] as shown in Figure 2.7. It is a circular patch with U-slot loaded with two switches at its edges. PIN diodes are used for switching in this design. Figure 2.7 explains the polarization realized at each switching states. However, in this design, going from one state to another, antenna matching is lost. That is why three matching stubs are added to the antenna feed. Each stub is connected or disconnected to the feed by a switch. By this, the antenna feed is also reconfigurable, and each switching state is accompanied by different matching circuit. Therefore, three more switches are needed in addition to the two switches on the antenna itself. Hence, integrating the biasing circuits for the total five switches of the antenna prototype is quite complicated. This complexity in the design limits its practical application for different wireless applications. Bandwidth achieved is around 2.6% and maximum gain is 6 dBi.

Lastly, in [26], CP is obtained by adding a perturbation tab to a circular patch antenna as shown in Figure 2.8. For reconifgurability, this tab is allowed to be connected or disconnected to the patch via PIN diode. The patch printed on the top layer is aperture coupled to a microstrip line feed on the bottom layer. The aperture has a ring shape carved on

the ground plane in the middle layer. For both LP modes an open stub is added to the antenna feed. The stub is enabled or disabled with another diode. Finally, ring slot is loaded with a third PIN diode for switching form vertical to horizontal LP. Antenna switching states are tabulated in Table 2.2. The proposed design has a wide bandwidth at each polarization mode, but they don't overlap together. Thus, the achieved overlapped bandwidth is narrow (2.24%). Also, the maximum gain obtained is 5.3 dBi. Furthermore, antenna structure is complicated. Since, it has three PCB layers and several design parameters, that yield deign complexity. The common drawback among the surveyed antenna designs is either the narrowband performance or complexity of the design.

2.3 RF Switching

For switching the polarization, PIN diodes are the commonly used switching devices for RF and microwave front-end application systems, because they have attractive properties such as low insertion loss, good isolation, ease of integration to PCB, fast switching speed, and low cost [27]. Figure 2.9 shows some commercial PIN diodes available in the market. Among the drawback of PIN diodes is the non-linearity for large signals, which in turn limits its usage for high power applications. On the other hand, RF-microelectromechanical systems (RF-MEMs) provide attractive switching features for high frequency systems [28]. Figure 2.10 shows a picture of RF MEMs switch.

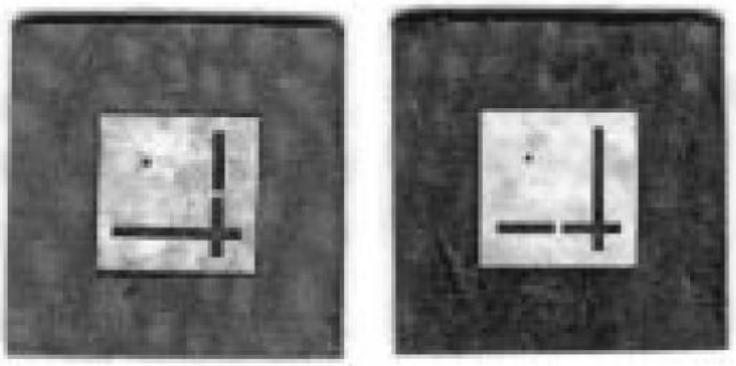

State 1 State 2

Figure 2.4 Reconfigurable microstrip antenna for switchable polarization [19].

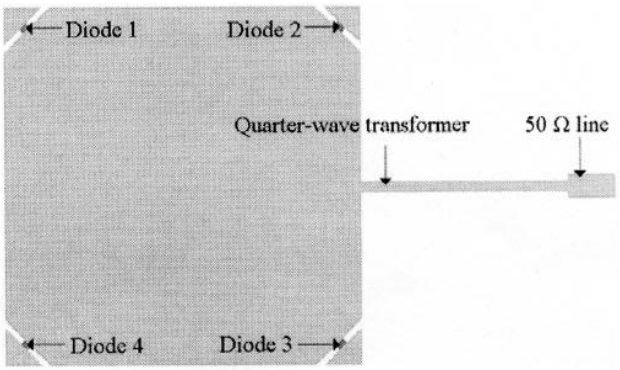

Figure 2.5 Reconfigurable microstrip antenna with switchable polarization [20].

Table 2.1 Antenna switching states [20].

Antenna	Diode 1	Diode 2	Diode 3	Diode 4	Polarization	Frequency [GHz]	BW [%]	Gain [dBi]
1	ON	ON	ON	ON	LP	1.579	1.84	5.3
2	OFF	OFF	OFF	OFF	LP	1.609	1.80	5.2
3	ON	OFF	ON	OFF	LHCP	1.599	2.57	5.3
4	OFF	ON	OFF	ON	RHCP	1.604	2.57	5.3

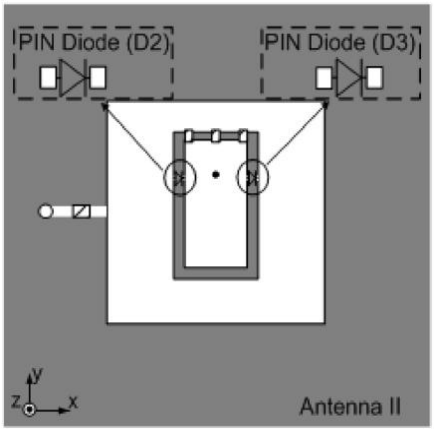

Figure 2.6 Reconfigurable U-slot antenna [19].

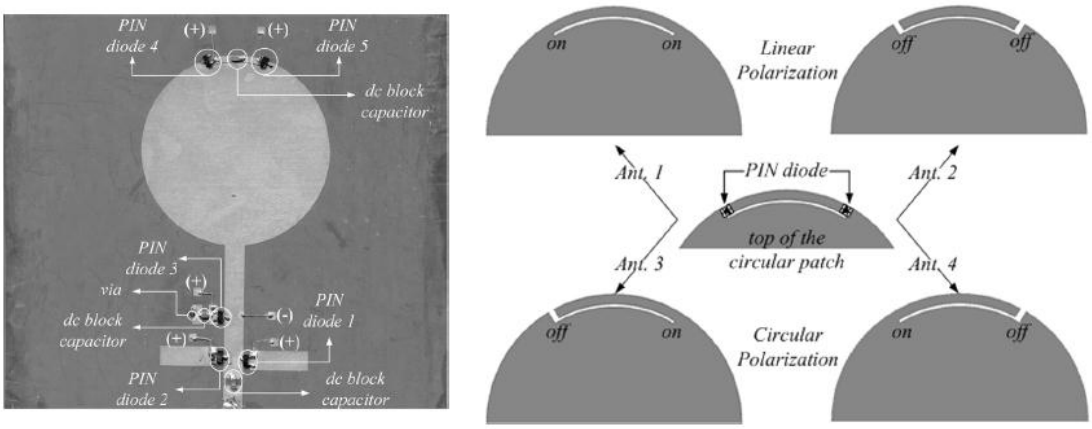

Figure 2.7 Reconfigurable circular patch with switchable polarization [19].

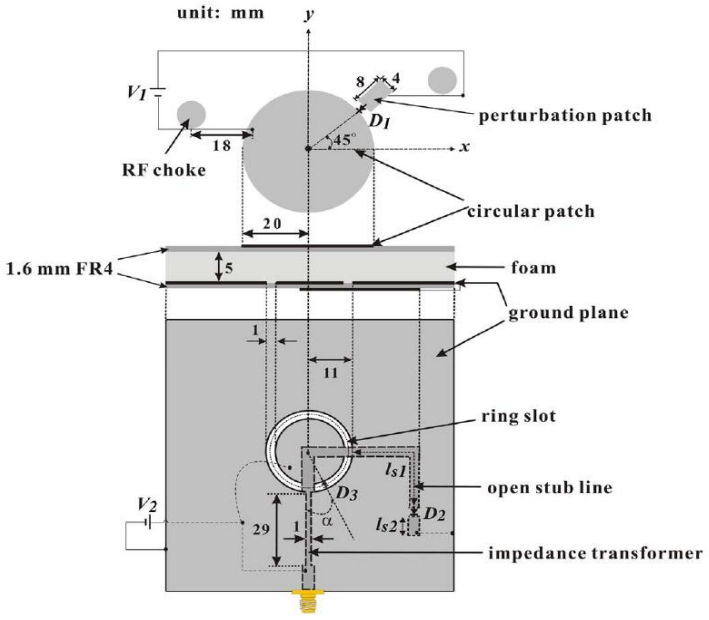

Figure 2.8 Reconfigurable microstrip antenna with quadruple switched polarization [19].

Table 2.2 Antenna switching states Table 2.2 [26].

diode state			polarization	operating bandwidth
D_1	D_2	D_3		
OFF	ON	ON	E_x	2365 - 2490 MHz
OFF	OFF	OFF	E_y	2380 - 2490 MHz
ON	ON	ON	E_{RHCP}	2430 - 2485 MHz
ON	OFF	OFF	E_{LHCP}	2390 - 2500 MHz

Figure 2.9 Different packages of RF PIN diode manufactured by Skyworks [28].

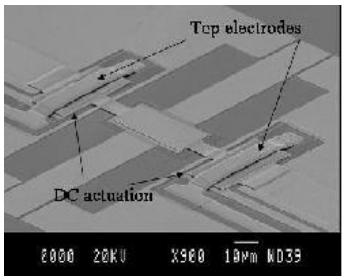

Figure 2.10 RF MEMs switch by the Laboratory for Analysis and Architecture of Systems: LAAS-CNRS [30].

2.4 Motivations

As seen in section 2.2, many proposed designs for polarization reconfigurable microstrip antennas, suffer from narrow bandwidth in CP modes, typically (2.7%) at most which is not satisfactory for some wireless applications such as WLAN IEEE802.11 b/g. Also, the realized gain doesn't exceed 6dBi, except for [24] which is 7.5dBi. Furthermore, matching the antenna at different polarization mode and controlling the RF PIN diodes that realize switching among them, requires complexity in the design which limits their practical application [25], [26].

The objective of this thesis is to design, fabricate, and test a polarization reconfigurable microstrip antenna with wide bandwidth (4% minimum) and high gain (6 dBi minimum). The design should be simple to be of practical interest in different existing wireless communication systems. For demonstration purpose, the design targets WLAN IEEE 802.11b/g (2.4-2.5GHz).

CHAPTER 3

CP E-SHAPED MICROSTRIP PATCH ANTENNA

3.1 Antenna Geometry and CP Mechanism

3.1.1 Antenna Configuration

The antenna geometry is shown in Figure 3.1. It consists of a modified E-shaped patch antenna with unequal parallel slots. Both slots have the same width (Ws). The patch outer dimensions are W and L. It is built over air substrate at height (h) from the ground plane. The antenna is fed with a coaxial probe at a distance (F) from the middle of the right edge of the patch as shown in Figure 3.1

3.1.2 The CP Design

The conventional E-shaped patch is shown in Figure 3.2 (a). Its radiation is linearly polarized and symmetric in the xz plane. To make this antenna circularly polarized, the x-directed current needs to be equal in magnitude to the y-directed current, with 90º phase difference. This is accomplished by making one of the slots in the E-patch shorter than the other. This introduces asymmetry in the xz plane which increases the x-directed current and its magnitude is almost equal to the y-directed current, as shown in Figure 3.2 (b). The antenna dimensions are then adjusted such that these two orthogonal currents are in phase

quadrature. It is instructive to present the vector current distribution on both optimized LP and CP E-shaped patch for various phase difference. Figures 3.3 and 3.4 show the current vector distribution on the CP and LP E-shaped patch at 2.45GHz.

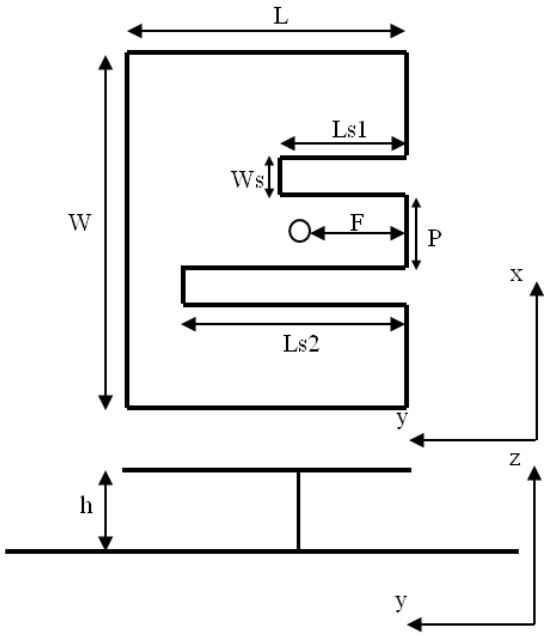

Figure 3.1 Antenna geometry.

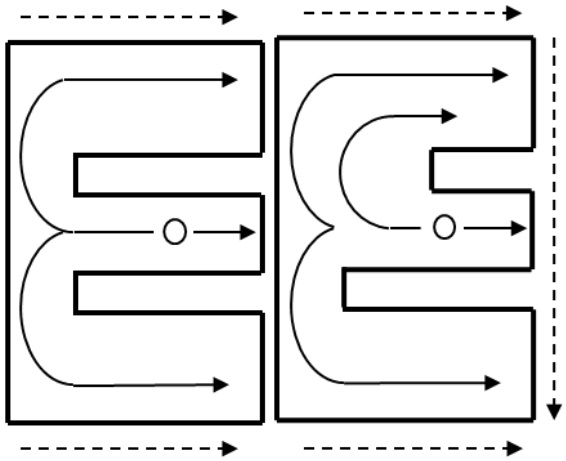

(a) (b)

Figure 3.2 Current flow across patch. (a) Linear polarized E-patch. (b) Circular polarized E-shaped patch.

Table 3.1 Dimensions of linear polarized E-shaped patch in mm

W	L	Ws	Ls1	Ls2	P	F	h
76	45	7	40	40	14	10	10

The zoomed part at 0º, 90º, 180º, and 270º phase states mimic current animations. From Figure 3.3, at 0º phase, the current flows in the y-direction, whereas, at 90º phase, the current flows in the x-direction. Similarly, at 180º and 270º, both currents are in opposite directions. This implies quadrature phase between currents in the x-and y-directions. Also, it is clear that the tips of the current vectors rotate in circular path with phase progression which depicts circular polarization. Therefore, it is expected that (L) and (W), together with the two slot lengths, control the resonant lengths of the x-and y-directed currents, respectively. That is why there is no need for the patch to be nearly square or corner trimmed. Instead, circular polarization is achieved by incorporating unequal parallel slots into the patch and adjusting their length, width, and position so that the phase difference between the orthogonal currents is 90º. On the other hand, at 0º, the current flows in the y-direction as shown in Figure 3.4. While at 90º and 270º, the current is almost zero due to cross polarization existence. Then at 180º, the current flows in the opposite direction of that of 0º. Thus, the tip of the current vector alternates between the '+' and '-' y-direction during one cycle.

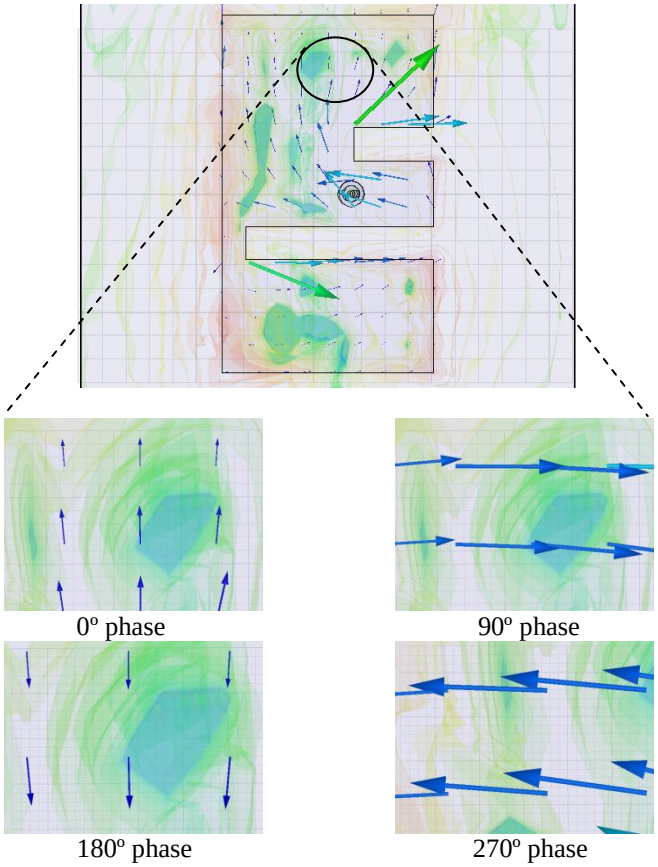

Figure 3.3 Current vector distribution on the CP E-shaped patch and zoomed part of it at different phase states.

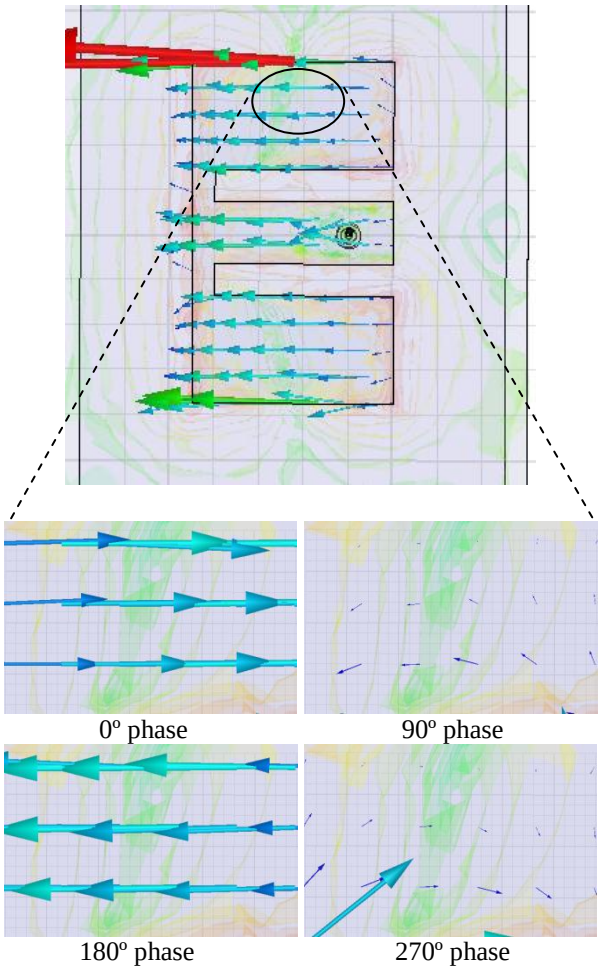

Figure 3.4 Current vector distribution on the CP E-shaped patch and zoomed part of it at different phase states.

This implies linear polarization. Next section shows how to adjust the antenna dimensions to obtain optimum performance and demonstrate the physical effect of various parameters.

3.2 Parametric Analysis and Design Procedure

3.2.1 Parametric Study

Basically, W and L control the resonant length of the x-and y-orthogonal currents excited across the patch edges, respectively. The incorporated parallel slots change the electrical length of both currents and hence they have significant effect on the resonant lengths. We start with the conventional linear polarized E-shaped patch to cover the 2.45GHz WLAN band. The dimensions of such an antenna are tabulated in Table 3.1. Details for

designing the E-shaped patch antenna at certain band are discussed in [19]. When slot Ls1 gets shorter, it is expected that the axial ratio will decrease. Figures 3.5 and 3.6 show the effect of Ls1 on S_{11} and AR, respectively, based on simulation results obtained using the Ansoft HFSS software package [30]. As expected, the shorter Ls1, the higher the resonant frequency. Also making Ls1 shorter improves the axial ratio drastically. It drops from values above 40dB at Ls1=40mm (case of linear polarization) to values around 7 dB at Ls1=20mm (elliptical polarization). Further decrease in the length of Ls1 will not improve AR anymore; rather AR begins to increase again. These are consistent results because Ls1 change the electrical path length of the x-directed current. At a certain length of Ls1, the electrical patch length of the x-directed current is such that its phase is 90^{o} different from that of the y-directed current. Beyond this specific value, the phase difference between the orthogonal currents retreats from 90º. It is found that the optimum value of Ls1, for the current antenna configuration, is 17mm which gives the minimum AR level.

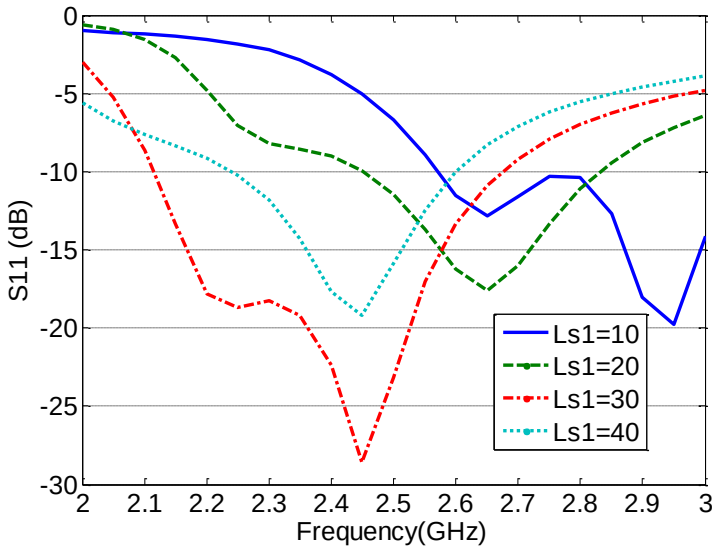

Figure 3.5 S_{11} at different values of Ls1 while the other parameters in Table 3.1 are fixed.

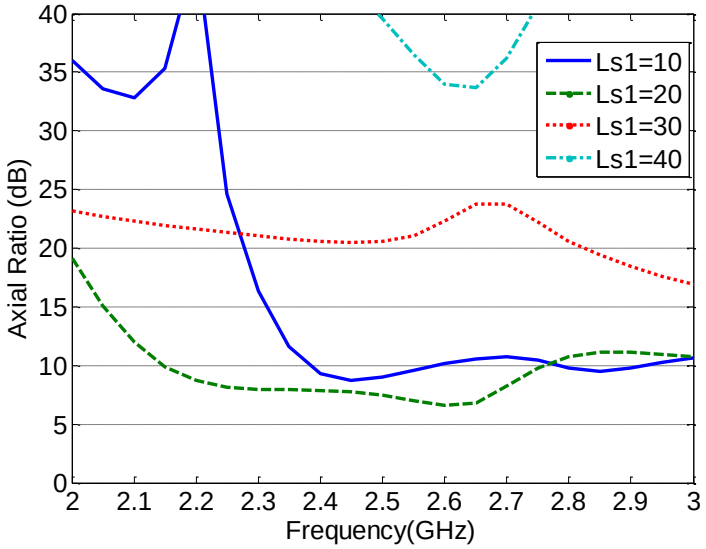

Figure 3.6 Axial ratio at different values of Ls1 while the other parameters in Table 3.1 are fixed.

The goals after this step are: (a) to improve the AR level as it is still far from the desired 3dB level; (b) to align the impedance and AR are bandwidths together. The probe position is expected to play a critical role for impedance matching as well as improving the AR level. Because its position changes the impedance seen by the source, it can improve matching to 50Ω. Effects of probe position on both S_{11} and AR are shown in Figure 3.7 and Figure 3.8, respectively. As expected at specific set of parameters, good matching and improved AR level could be aligned together within the band of interest.

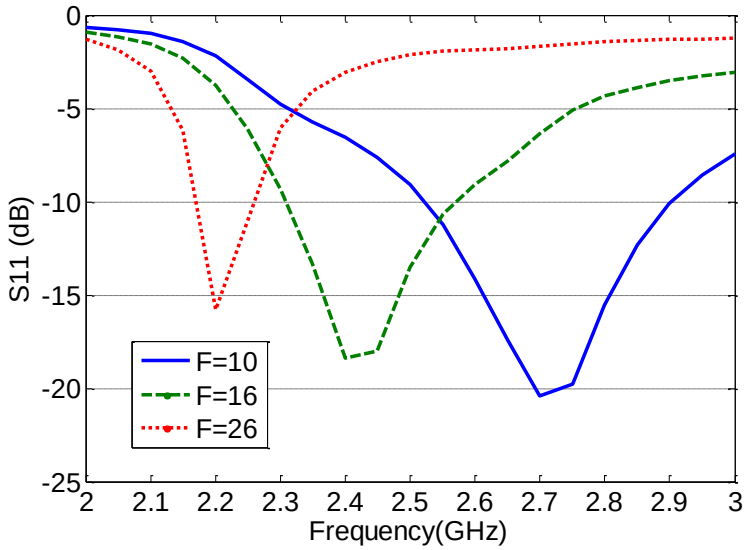

Figure 3.7 S_{11} at different values of F and Ls1=17 mm while the other parameters in Table 3.1 are fixed.

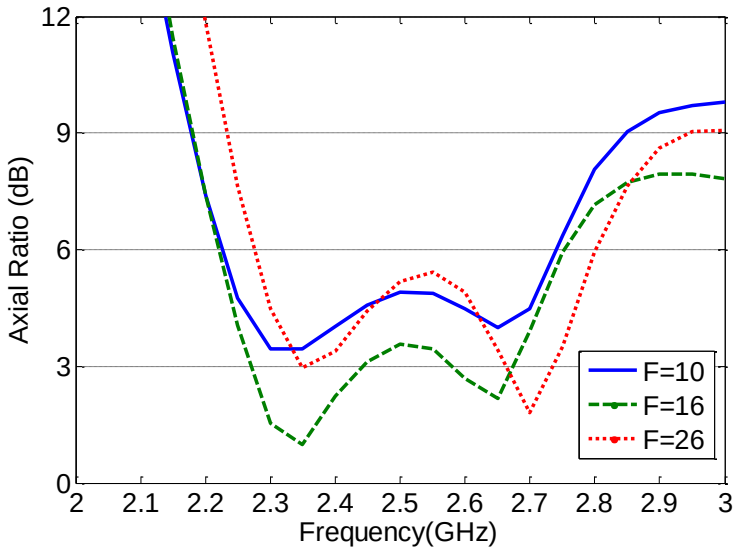

Figure 3.8 Axial ratio at different values of F1 and Ls1=17 mm while the other parameters in Table 3.1 are fixed.

According to the above discussion it is expected that Ls2 can be effective as Ls1, because it changes the x-directed current electrical path length and hence affect both S_{11} and AR level in a similar fashion. Figure 3.9 shows the effect of Ls2 on S_{11}: as expected, when Ls2 increases the resonant frequency decreases and vice versa. Whereas, Figure 3.10 shows

its effect on the AR is similar to that of Ls1, but it is observed that Ls2 is less sensitive, which could be useful for fine tuning the S_{11} band and AR improvement.

3.2.2 Design Procedure

Based on the above parametric study and discussion the following systematic design procedure is proposed:

Step 1) Start with LP E-shaped patch covering the band of interest as given in [6]. It is not necessary to optimize the design for maximum obtainable impedance bandwidth, because this will be distorted later by changing one of the slot dimensions.

Step 2) For LHCP, begin with making the length of Ls1 shorter (while Ls2 fixed) untill minimum AR level is obtained. Opposite procedure should be followed if RHCP is required.

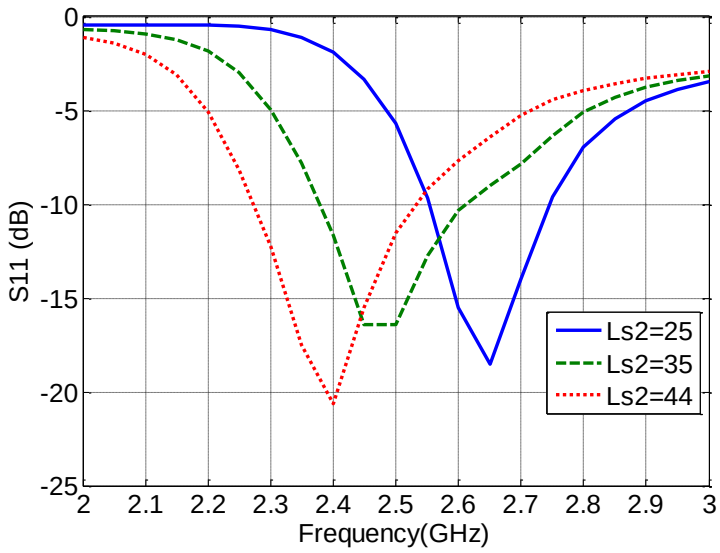

Figure 3.9 S_{11} at different values of Ls2 while Ls1=17 mm, F=16 mm, and other parameters in Table 3.1 are fixed.

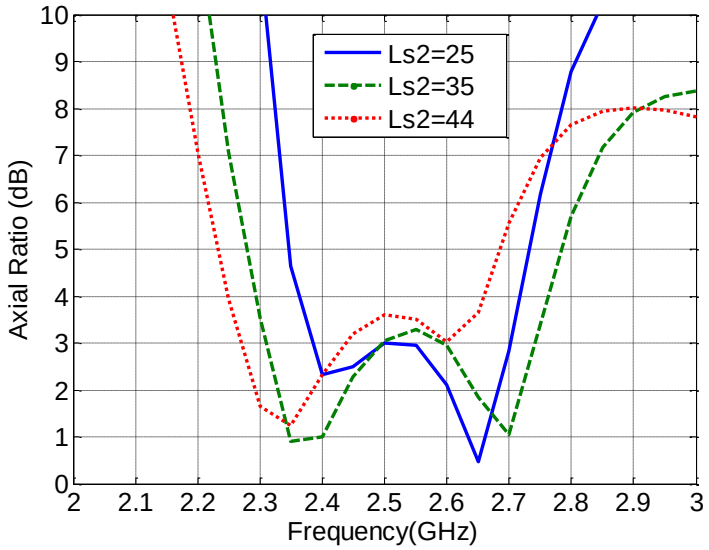

Figure 3.10 Axial ratio at different values of Ls2 while Ls1=17 mm, F=16 mm, and other parameters in Table 3.1 are fixed.

Step 3) Change the probe position along the y direction for improving the AR level as well as aligning the S_{11} band with the AR band.

Step 4) As a last step Ls2 could be changed for fine enhancement of AR level as well as alignment with S_{11} band.

Figure 3.11 shows a flowchart for the suggested design and tuning procedure. The previous procedure could be repeated iteratively until satisfactory results are obtained. Moreover, in the next loop Ls1 could be increased or decreased rather than decreasing only as in the first loop. The same applies to the other parameters.

3.3 Design Examples and Comparison with CP U-Slot Antenna

In this section, CP E-shaped patch is designed using the above suggested procedure on two different substrate materials with different thicknesses. Antenna performance is compared with the two recently published CP U-slot patches in [17]-[18].

3.3.1 Design I

The geometry of the antenna is the same as in Figure 3.1, while the geometrical parameters of the CP U-slot antennas are shown in Figures 3.12 and 3.13, respectively. Air substrate with 10mm ($0.08\lambda_o$) thickness is used. The optimized dimensions of the designs for operation at IEEE 802.11b/g band (2.4-2.5GHz) are tabulated in Tables 3.2, 3.3, and 3.4. Figure 3.14 shows S_{11} of the three antennas. From the results E-patch exhibit 10.1% impedance bandwidth (2.35-2.6GHz), while unequal arms U-slot has 9.25% (2.37-2.6GHz) and the truncated corner U-slot has 9.64% (2.27-2.5GHz). Axial ratio of the three antennas is shown in Figure 3.15. It is clear that all AR bandwidths are aligned with the corresponding S_{11} bandwidth. Axial ratio bandwidth inherent with the E-patch is 6.5% (2.38-2.54GHz) which is pretty wide for a single-layer single-feed microstrip antenna. Also, 4% (2.39-2.49GHz) AR bandwidth is obtained from unequal arms U-slot while 4.5% (2.39-2.2.5 GHz) from truncated corner U-slot. This shows that the proposed design produces CP fields with wide AR bandwidth, which is comparable to other techniques such as using U-slots.

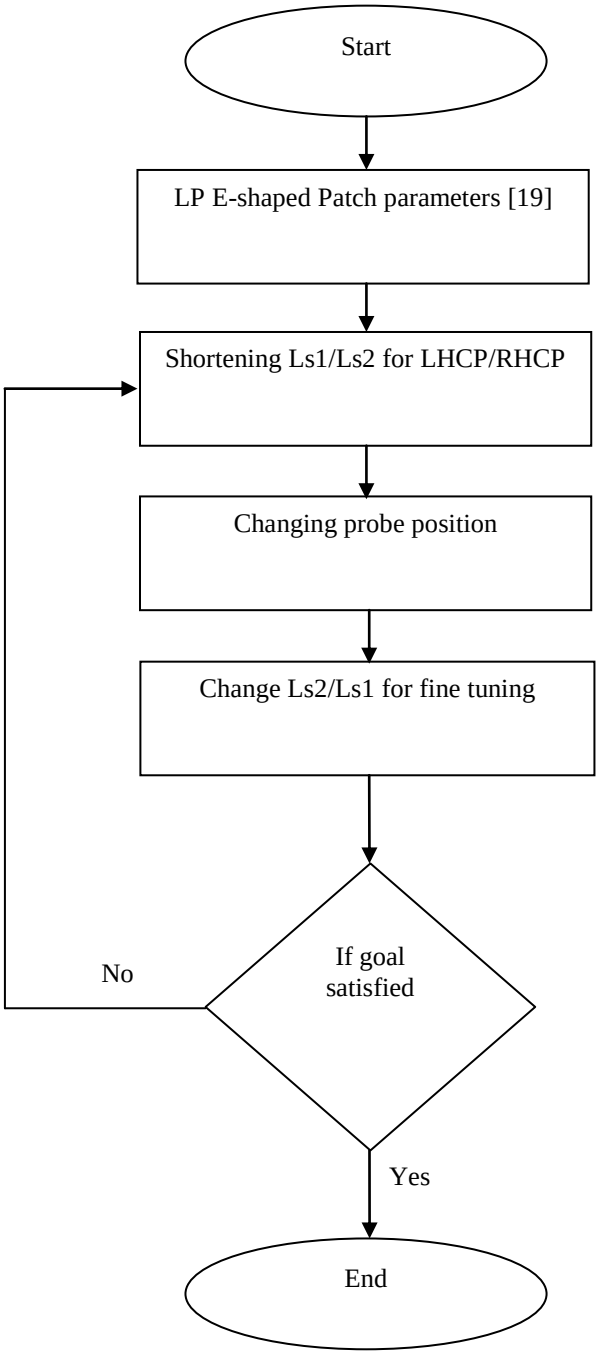

Figure 3.11 Flow chart for the design and tuning procedure.

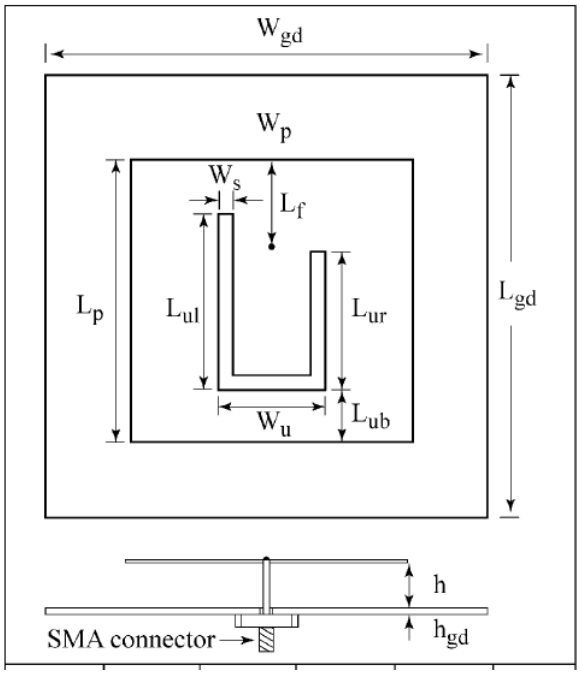

Figure 3.12 Geometry of CP unequal arms U-slot antenna [17].

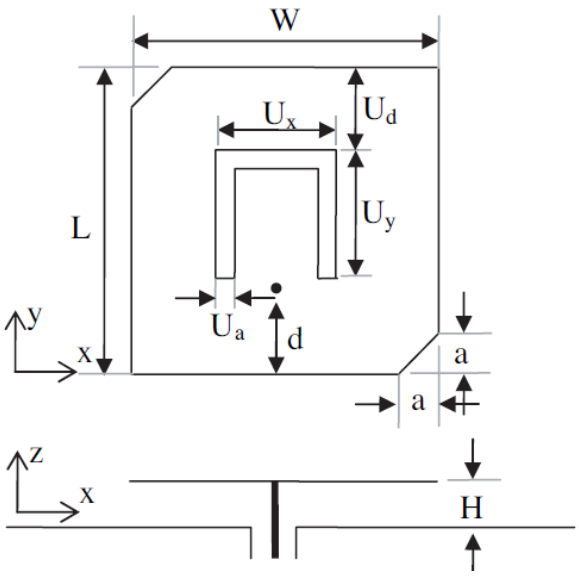

Figure 3.13 Geometry of CP truncated corners U-slot antenna [18].

Table 3.2 Dimensions of CP E-shaped patch in mm

ε_r	H	W	L	Ws	Ls1	Ls2	P	F
1	10	77	47.5	7	19	44.5	14	17
2.2	6.7	63	33.5	4	27	6	20	10

Table 3.3 Dimensions of CP unequal U-slot patch in mm

ε_r	H	L_p	W_p	L_{ul}	L_{ur}	L_{ub}	W_u	W_s	L_f
1	10	43.7	43.7	27.3	19.8	10.3	16.9	2.3	12.5
2.2	6.7	32.7	32.7	20	13.5	8.9	11.4	1.5	12

Table 3.4 Dimensions of CP truncated corner U-slot patch in mm

ε_r	H	L	W	a	d	U_a	U_d	U_x	U_y
1	10	48.2	48.2	12.2	10	2.1	19.8	23	19
2.2	6.7	36	36	7.7	6.5	1.2	19.6	15.5	11.5

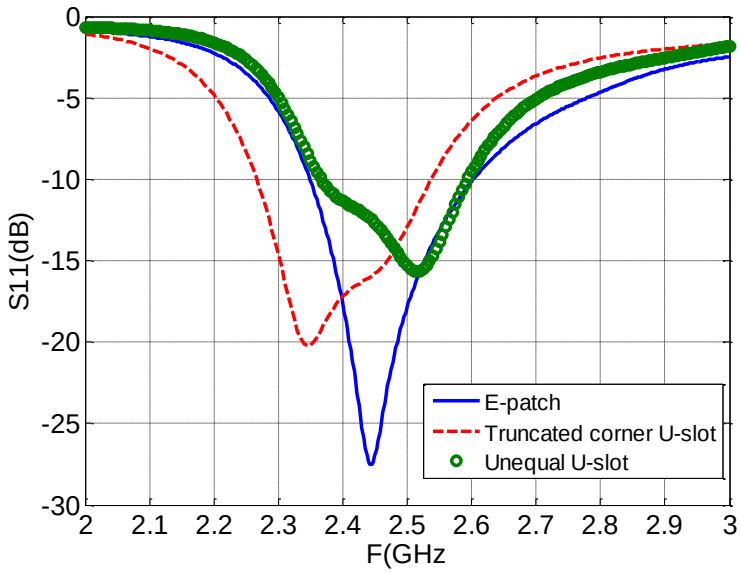

Figure 3.14 S_{11} for E-shaped, unequal arms U-slot, and truncated corners U-slot antennas.

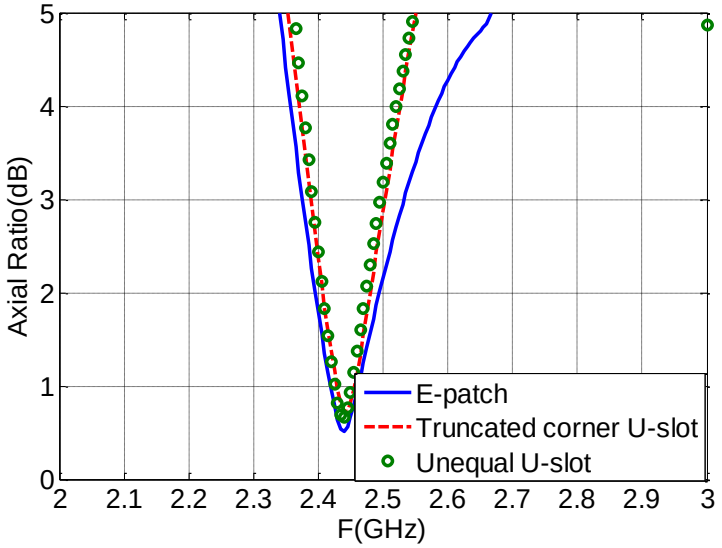

Figure 3.15 Axial ratio for E-shaped, unequal arms U-slot, and truncated corners U-slot antennas.

3.3.1 Design II

To show that the proposed design also works for material substrate, we use a substrate with ε_r=2.2 and thickness 6.7mm ($0.08\lambda_g$). The optimized dimensions are listed in Tables 3.2, 3.3, and 3.4. The results are shown in Figures 3.16 and 3.17. The modified E-shaped patch provides 10.6% (2.39-2.66GHz) impedance bandwidth and 3.6% (2.41-2.5GHz) AR bandwidth which is wider than expected with such permittivity.

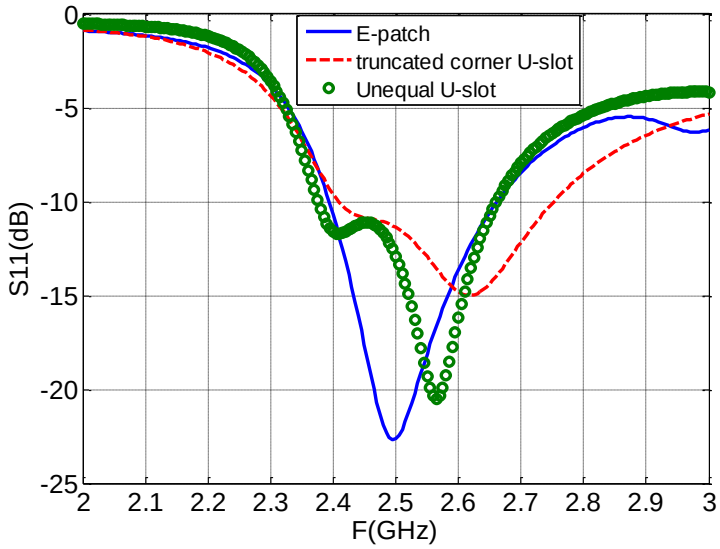

Figure 3.16 S_{11} for E-shaped, unequal arms U-slot, and truncated corners U-slot antennas.

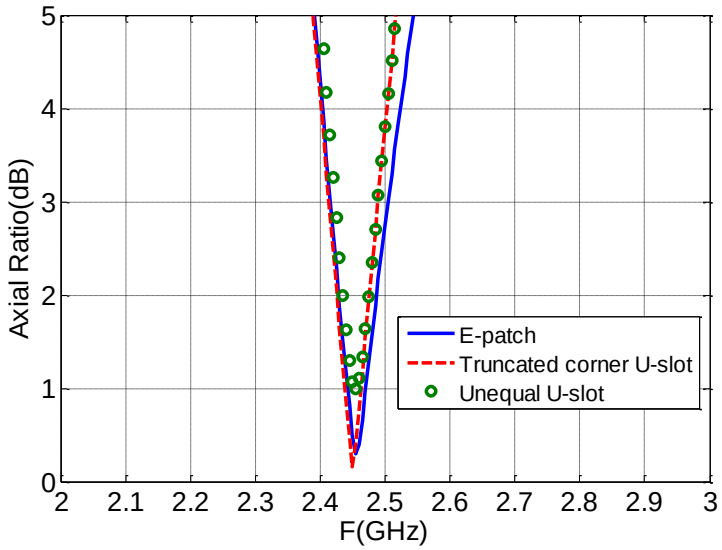

Figure 3.17 Axial ratio for E-shaped, unequal arms U-slot, and truncated corners U-slot antennas.

On the other hand unequal arms U-slot gives 6.9% (2.38-2.55GHz) impedance bandwidth and 2.8% (2.415-2.465 GHz) AR bandwidth, while truncated corners U-slot gives 13.1% (2.41-2.75GHz).

3.4 Fabrication and Measurements of CP E-Shaped Patch Antenna

"Design I" has been chosen for fabrication and measurements. Photo of the prototype is shown in Figure 3.18. The metallic patch is fabricated via milling a thin copper clad substrate. This enable etching the E-shaped patch dimensions with higher accuracy. The substrate layer has ε_r=2.2 and 0.787 mm thickness. It is mounted above a ground plane whose dimensions are 95 x 200 mm via a pin of 0.75 mm radius. Excitation pin is then soldered to a 50Ω SMA connecter as shown in Figure 3.18(b). Optimized dimensions are tabulated in Table 3.5.

Simulation and measured results of S_{11} are shown in Figure 3.19. Good agreement between simulation and measurement is observed. Measured antenna impedance bandwidth is 9.27% (2.34-2.57GHz), while 10.27% (2.31-2.57GHz) is obtained from simulation. Axial

ratio simulation and measured results are shown in Figure 3.20. It should be pointed out that the axial ratio simulation results do not satisfy the design requirements completely. Although the AR band is broad, (2.28-2.45GHz or 8.1%), it is slightly shifted downward from the band of interest (2.4-2.5GHz). We stopped the optimization run at these results because from experience we know that there is always some frequency shift in the measurements. This turned out to be the case, as the measured curve is shifted upward and satisfy the designed requirement. Moreover, it is observed that the measured AR bandwidth is 16% (2.3-2.7GHz). The overlapped bandwidth between S_{11} and AR is 2.34-2.57GHz which is 9.27%.

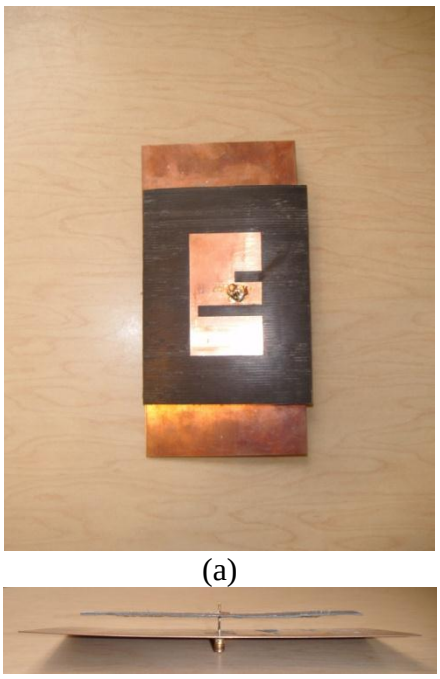

(a)

(b)

Figure 3.18 Prototype of CP E-shaped patch antenna (a) plane view, (b) side view.

Table 3.5 Dimensions of CP E-shaped patch prototype in mm

W	L	Ws	Ls1	Ls2	P	F	h
76	45	7	40	40	14	10	10

The LHCP vs. RHCP patterns in yz and xz planes at 2.45GHz are shown in Figure 3.21. Gain versus frequency in the broadside direction is shown in Figure 3.22. Maximum measured gain obtained is 8.3dBi with 3dB bandwidth 2.27-2.65GHz (15.5%), against maximum simulated gain of 8.7dBi with 3dB bandwidth 2.18-2.65GHz (19.5%). The overlapped bandwidth among impedance, AR and gain is 9.27% which is the effective bandwidth of the antenna. This is considered a very wideband for a single-feed single-layer microstrip antenna.

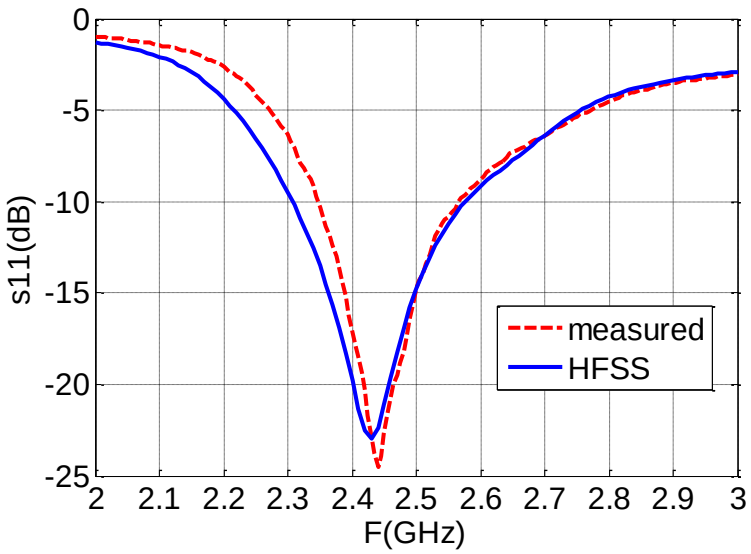

Figure 3.19 Simulation vs. measurements of S_{11} for CP E-shaped patch antenna.

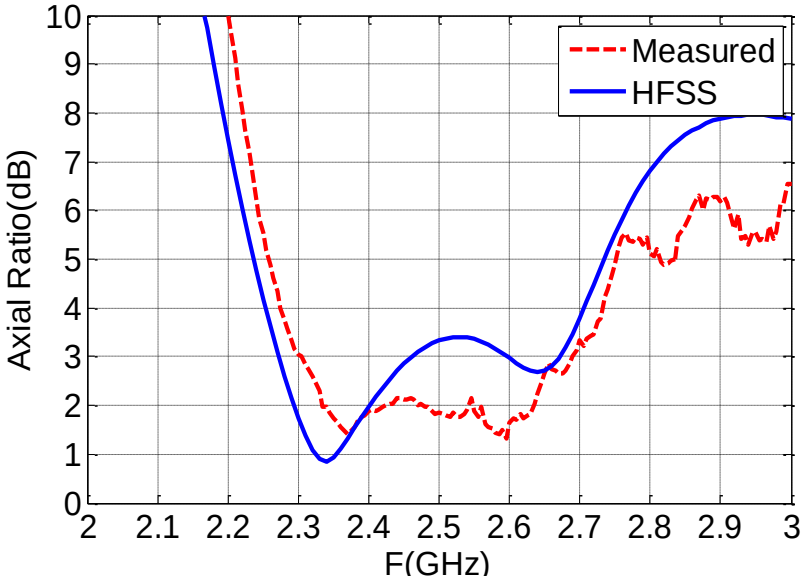

Figure 3.20 Simulation vs. measurements of axial ratio for CP E-shaped patch antenna.

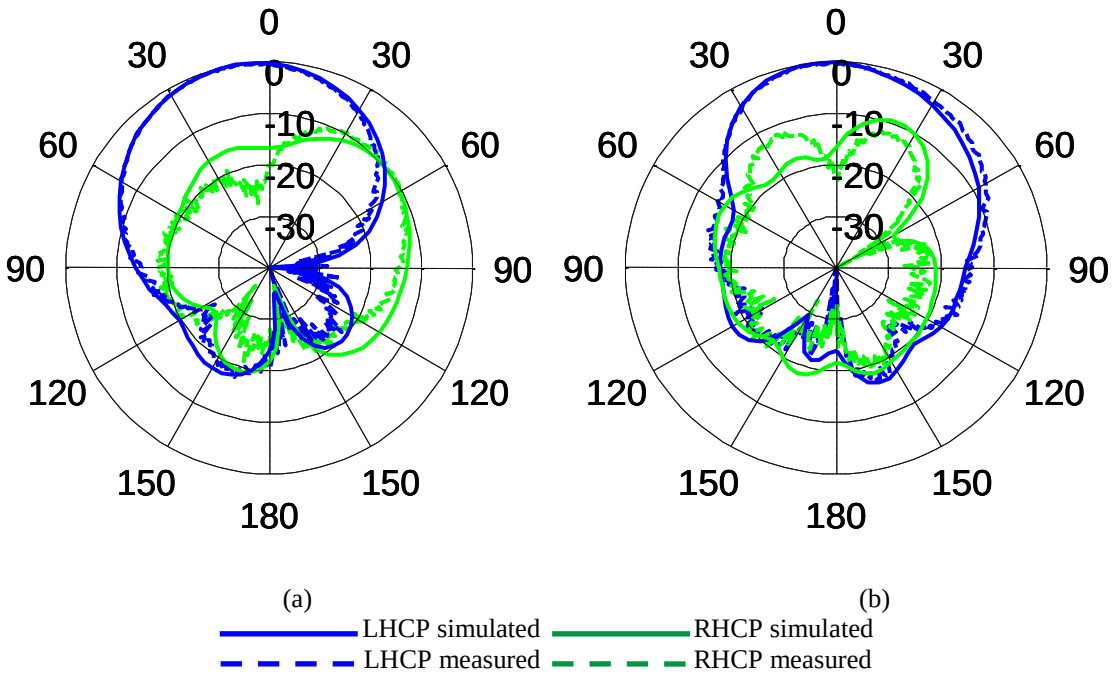

Figure 3.21 Radiation pattern of circular fields at 2.45GHz (a) yz (b) xz.

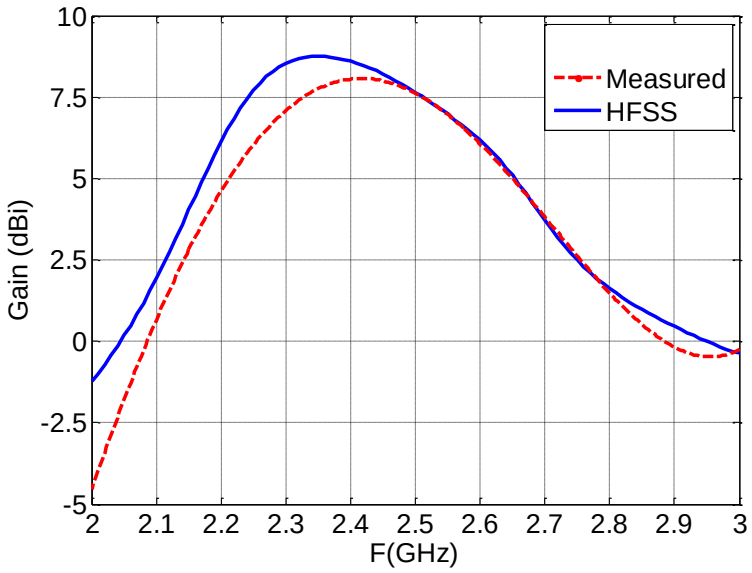

Figure 3.22 Simulation vs. measured broadside gain versus frequency.

CHAPTER 4

RECONFIGURABLE E-SHAPED PATCH ANTENNA

4.1 Principle of Operation

When an E-shaped patch antenna is loaded with two switches, one on each of its slots as shown in Figure 4.1, the antenna will have four possible switching states as listed in Table 4.1. At state 1, the E-shaped patch would resonate at 'f_L' and radiate linear polarized (LP) fields [14]. At state 2, the two switches are ON which allows the surface currents to pass through them, making the current path becomes shorter. Thus, the electrical length is smaller and the antenna would resonate at higher frequency 'f_H' ($f_H > f_L$). Due to the symmetry of the antenna structure, at state 2, the polarization would also be linear. Consequently, going from state 1 to state 2 or the vice versa is a frequency reconfigurable E-shaped patch antenna with linear polarization. The resonant frequency in both states 1, 2 is 'f' ($f_L < f < f_H$). On that ground, wideband polarization reconfigurable E-shaped patch antenna is realized.

Recently, it has been shown that CP fields could be excited with E-shaped patch antenna with wide effective bandwidth (9.27%) [32]. Letting one of its slots shorter than the other, would introduce asymmetry and perturb the field beneath the patch, thus producing CP fields. Therefore, E-shaped patch antenna at state 3, effectively has the upper slot shorter than the lower one. At appropriate position of the switch, LHCP could be attained. In a similar

fashion, state 4 yields RHCP. The current distribution of E-shaped patch antenna in state 3 is shown in Figure 4.2, where the current rotates clockwise which implies LHCP.

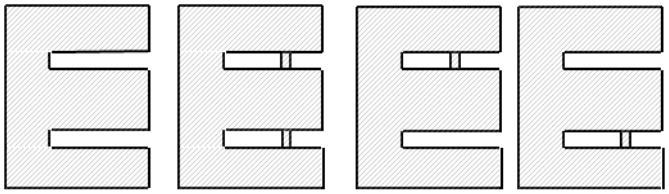

(a) (b) (c) (d)

Figure 4.1 Switching states of the E-shaped patch antenna (a) state 1 (b) state 2 (c) state 3 (d) state 4.

Table 4.1 Antenna possible configurations

State	SWITCH 1	SWITCH 2	FREQUENCY	POLARIZATION
1	ON	ON	f_L	LP
2	OFF	OFF	f_H	LP
3	ON	OFF	f	LHCP
4	ON	OFF	f	RHCP

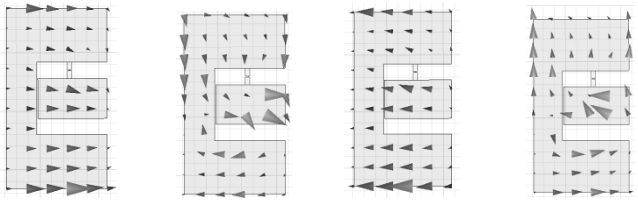

t=0 t=T/4 t=T/2 t=3T/4

Figure 4.2 Current distribution on E-shaped patch antenna in state 3.

4.2 Antenna Geometry

The reconfigurable E-shaped patch antenna geometry is shown in Figure 4.3. The design follows the procedure in [32]. Single fed E-shaped patch antenna is printed on a thin sheet of RT/duroid 5880 dielectric substrate with ε_r=2.2 and thickness t=0.787mm. The substrate is mounted 10mm above the ground plan, by coaxial feed pin. Although the antenna is required to be built over air substrate, the dielectric substrate facilitates mounting the microwave components on the antenna surface, as well as printing short stub. Two RF PIN diodes are inserted on each slot of the E-shaped patch antenna. For the two diodes to function

as RF switches, they need to be biased by a DC voltage source. To avoid DC short across the diodes terminals, a narrow slit of width s=0.5mm is incorporated on the E-shaped patch surface, to divide it into two parts: part 1 and part 2. However, to maintain the performance at RF frequencies, three DC block capacitors are inserted on the narrow slit. Therefore, at DC the E-shaped patch has two isolated metallic parts; hence, no DC short would occur on biasing the diodes. Whereas, at RF frequencies, the E-shaped patch would be one metallic part and performance is preserved. Part 2 of the E-shaped patch is DC grounded through a vertical via connected to it by a narrow λ/4 transmission line. This ensures high impedance (ideally open circuit) at the edge of the E-shaped patch. Hence, the current distribution on the E-shaped patch is kept unperturbed at RF frequencies. The ground plane is common for both the DC and the RF signals. Its size is 200 × 100 mm.

The RF and DC positive (+) signals are supplied to the antenna via the coaxial pin feed. They are superimposed together through the bias tee for RF/DC isolation. Part 1 is positive (+), and part 2 is grounded. Thus, the D2 diode would be ON, whereas the D1 diode would be OFF. The capacitors will block the DC current to go from part 1 to part 2 but allow RF current to go through them. RHCP is realized in this switching state. For LHCP, the terminals of the DC source have to be reversed, hence the D1 diode would be ON and the D2 diode would be OFF.

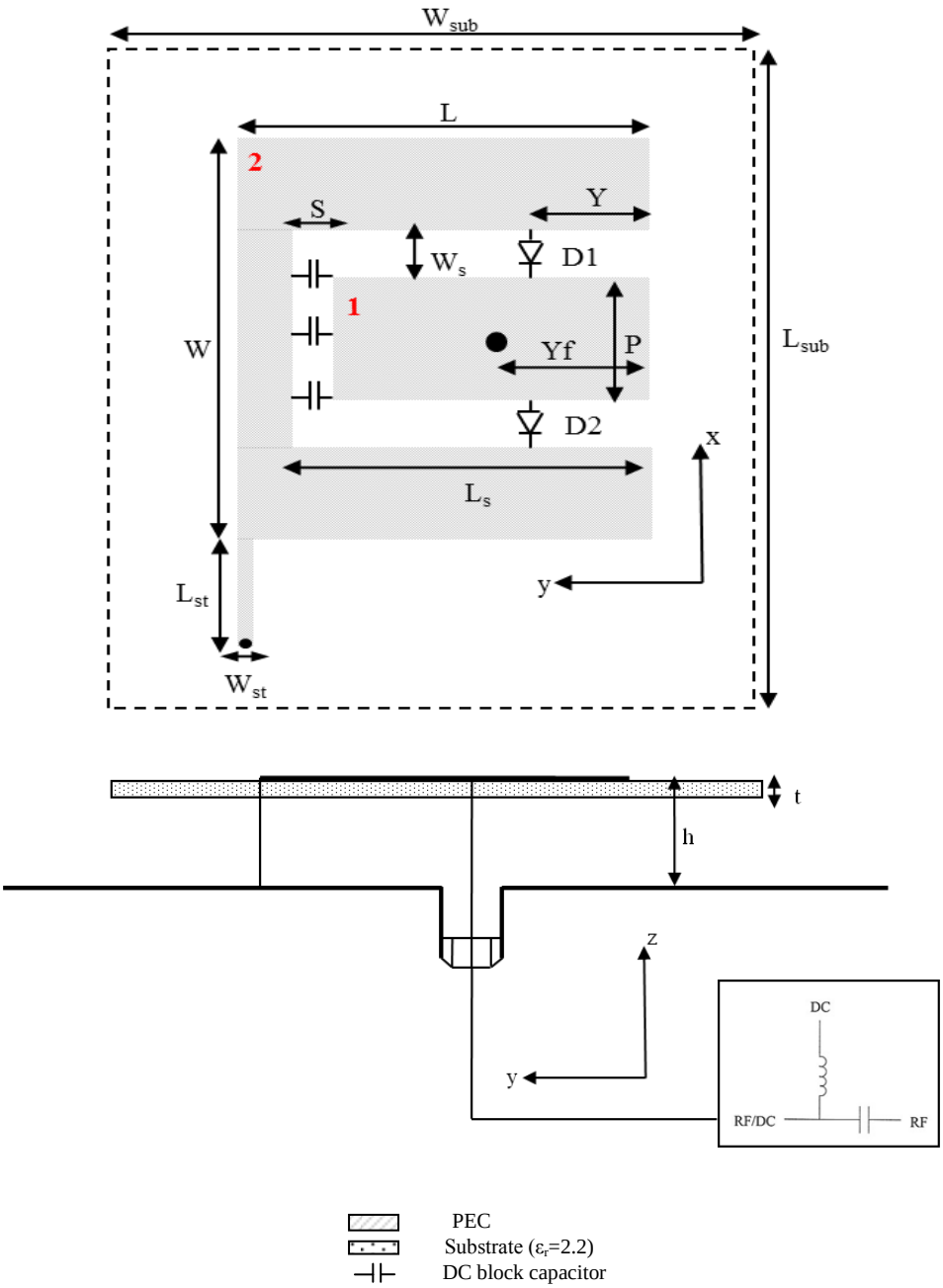

Figure 4.3 Geometry of a single feed reconfigurable E-shaped patch antenna with integrated DC biasing circuit. (a) Top view. (b) Side view. L_{sub} =140mm, W_{sub} =80mm, L=43mm, W=77mm, L_s=30mm, W_s=7mm, Y_f =14mm, P=17mm, L_{st} =28mm, W_{st} = 0.3mm, S=0.5mm, h=10mm, t=0.787mm.

4.3 Biasing Circuitry and Simulation Results

4.4.1 DC Block Capacitors

As discussed in section II.B, the capacitors role is to block the DC current on the E-shaped patch surface, and behave as a short circuit at RF frequencies. For this purpose, a setup of 50Ω microstrip transmission line with narrow slit at the middle of width 0.5mm was built as shown in Figure 4.4. A 10pF capacitor of model number ATC600F100 by A.T. Ceramics [33], is mounted on the narrow slit as shown in Figure 4.5. Selection of this capacitor was with the help of [34]. The measured S-parameters are shown in Figure 4.6. From the figure, the insertion loss is -0.03dB across the entire 2-3GHz band. This means, the band 2-3GHz is within the pass band of the capacitor and away from any of its self resonant frequencies [35]. Hence, at RF frequencies, these capacitors would not load the antenna with reactance and would not shift its resonant frequency.

4.4.2 RF PIN Diode Switch

Ideally, it is desired for an RF switch to have zero forward resistance in the ON state and infinite reverse impedance in the OFF state. However, in practice it always has a small finite forward resistance, and large finite reverse impedance.

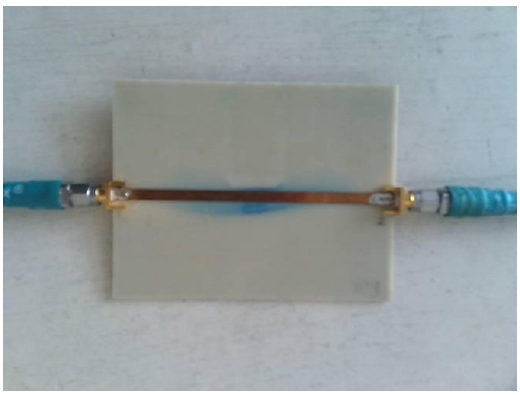

Figure 4.4 A 50Ω microstrip line with a narrow slit of 0.5 mm at the middle of it for characterizing the DC block capacitors and RF PIN diode switch.

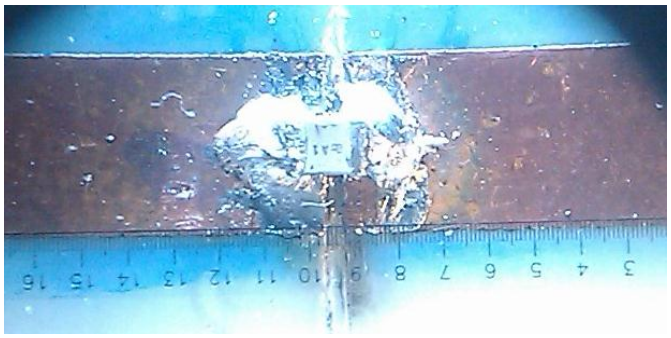

Figure 4.5 Magnified picture of the capacitor ATC600F100, mounted over 50Ω transmission line.

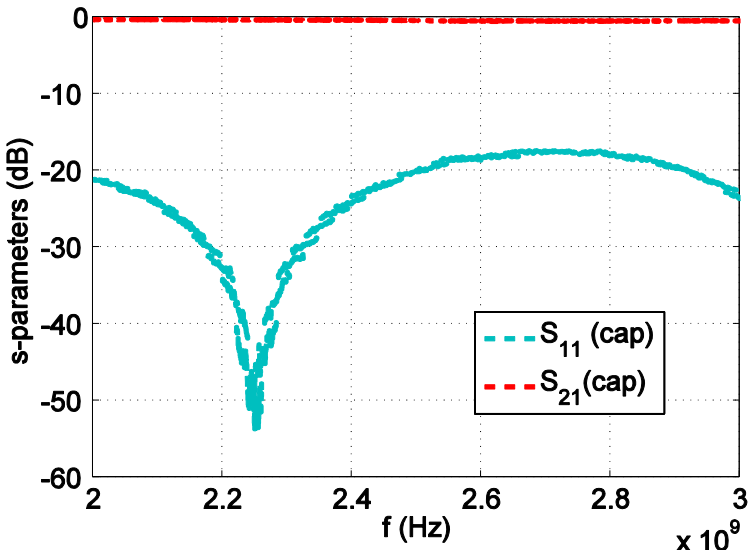

Figure 4.6 Measured S-parameters of the capacitor ATC600F100 mounted over a 50Ω transmission line.

Because, the diode will be mounted on a resonant structure, it is required in the OFF state, to have small parasitic capacitance (~0.05pF) to avoid frequency shift that leads to miss alignment between the axial ratio and the impedance band width. Also, forward resistance is required to be as small as possible (~5Ω) to avoid reduction in antenna gain. Commercial MA4SPS402 PIN diode manufactured by M/A-Com is used, since it satisfies these requirements. Its equivalent linear circuit model is extracted from its data sheet [36] and shown in Figure 4.7. At the ON state, it has 5Ω forward resistance. However, the value of this resistance is a function of the diode's forward current 'I_f'. Whereas, at the OFF state, it has

40kΩ resistor parallel with 0.03pF capacitor. These values have small variation with the reverse biasing voltage within 2-3GHz. The diode equivalent circuit model is used in full-wave simulation. It should be pointed out that, series parasitic inductance due to chip packaging, is neglected here for simplicity, since it is very small (~0.5nH).

A setup similar to the one used for the block capacitor, is used for the PIN diode as shown in Figure 4.8. Two bias tee were added at each port, and a DC voltage source 'V' in series with an arbitrary lumped resistor 'Rs' to control the forward biasing current 'I_f'. PIN diode is operated with a forward DC biasing voltage V_F=0.94V, and I_F=13.6 mA. Figure 4.9 shows a magnified picture of the PIN diode (MA4SPS402) mounted on a 50Ω transmission line. The measured insertion loss of the switch is -0.03dB in the ON state as shown in Figure 4.10.

Also, it is useful to measure the diode's linearity, which limits the power capability of the antenna. Figure 4.11 shows the measured power transfer relation using the same setup. Input power range is from 0.01mW (-20dBm) to 316 mW (25dBm). This range is limited to the facilities available in our lab. From Figure 4.11, it is obvious that up to 300mW input power, the transfer relation is linear. Hence, avoiding signal distortion during antenna operation.

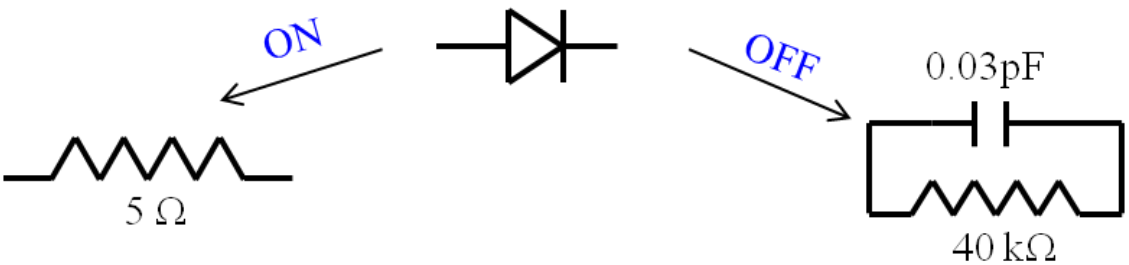

Figure 4.7 The linear circuit model of the PIN diode (MA4SPS402) in both ON/OFF states used in simulation at I_f =10mA.

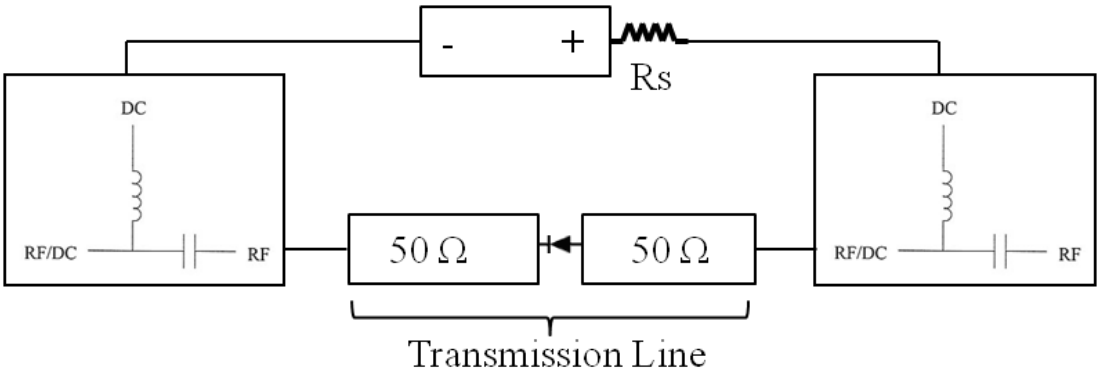

Figure 4.8 Setup for PIN diode insertion and return loss measurements.

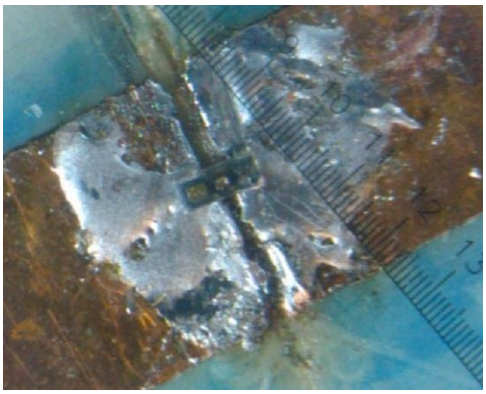

Figure 4.9 Magnified picture of PIN diode (MA4SPS402) mounted over 50Ω microstrip line for characterization.

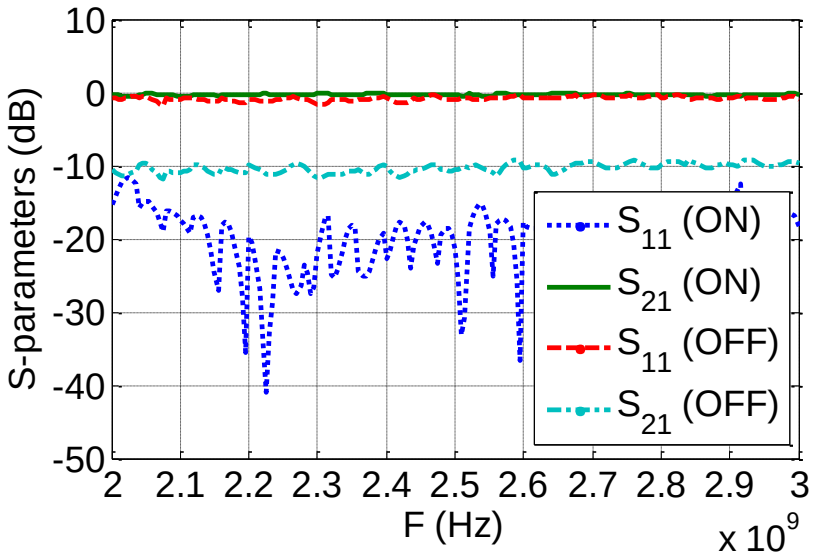

Figure 4.10 Insertion loss for the MA4SPS402 PIN diode, at I_f=10mA, V_f =0.94 V using 50 transmission line setup.

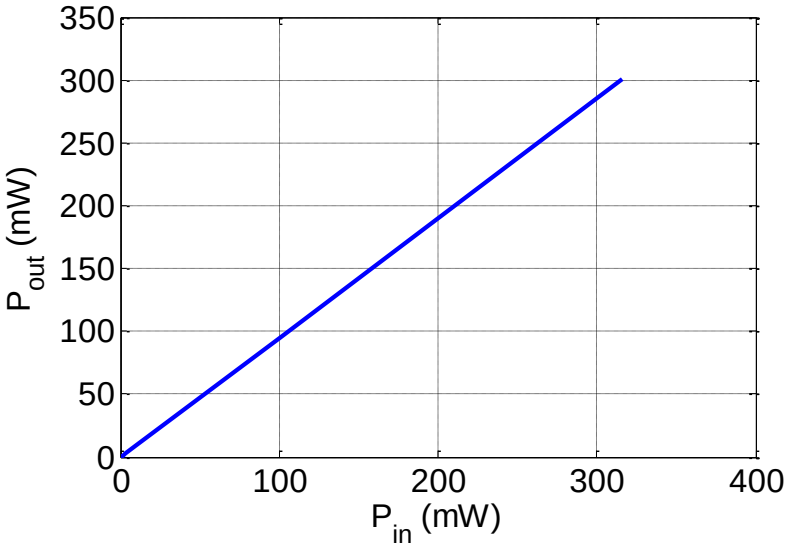

Figure 4.11 Power transfer relation of MA4SPS402 PIN diode using 50Ω transmission line setup.

4.4.3 Simulation Results

Full-wave simulation is carried out for the geometry in Figure 4.3 using Ansoft HFSS [30]. The diodes are modeled as in Figure 4.7. The results for S_{11} and axial ratio at different switch positions 'Y' are shown in Figure 4.12 and Figure 4.13, respectively. It is observed that, diodes position affects axial ratio within 2.4-2.5GHz band. Whereas, the effect on S_{11} is less significant, since at all positions it is less than -10dB within 2.4 - 2.5 GHz. Best diode position is at Y=13mm, where 8% overlapped impedance and axial ratio bandwidth is attained.

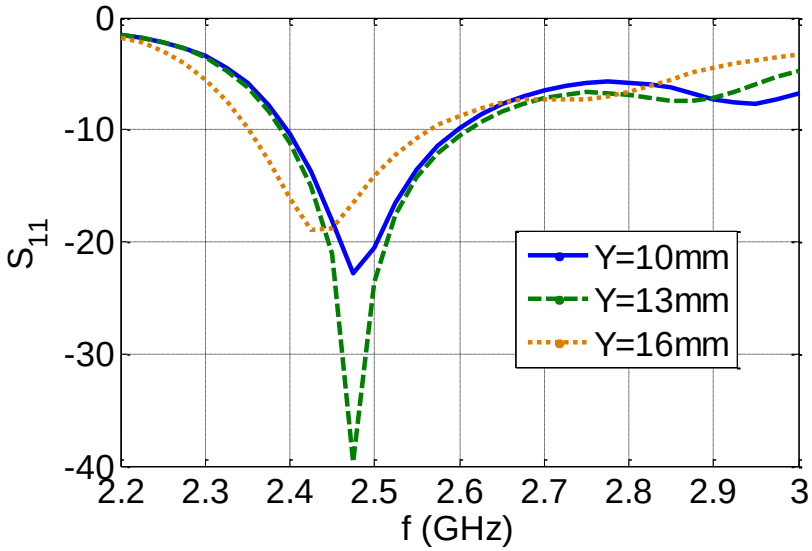

Figure 4.12 Simulation results for S11 of the reconfigurable E-shaped patch antenna in state 3 at different diodes' locations.

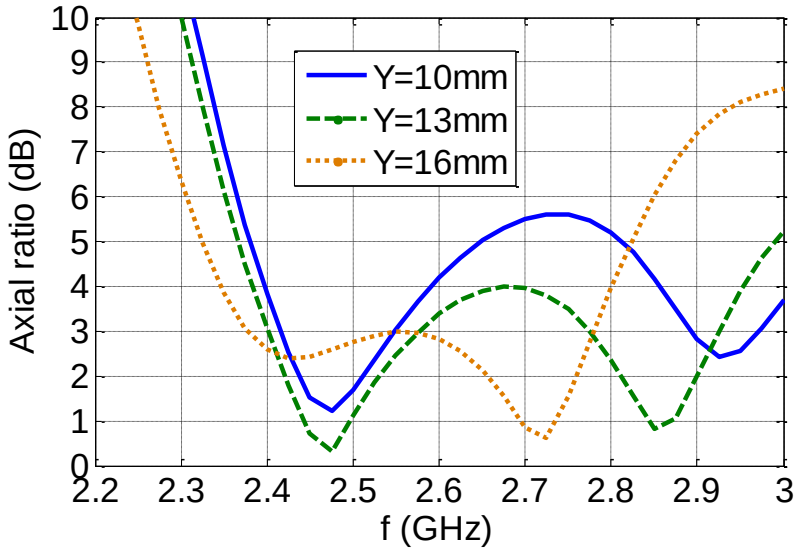

Figure 4.13 Simulation results for axial ratio of the reconfigurable E-shaped patch antenna in state 3 at different diodes locations.

4.4 Antenna Prototype and Experimental Verification

Figure 4.14 shows a picture of a fabricated antenna prototype, soldered on it the block capacitors and PIN diodes. A 10mm thick foam brick is inserted between the ground plane and the dielectric substrate as a support. Metallic pads are printed on the slots to allow

mounting the PIN diodes. Simulated versus measured results of S_{11} and axial ratio in both switching states 3, 4 are shown in Figure 4.15 and Figure 4.16, respectively. Good agreement between simulated and measured results is observed. Due to the structure symmetry, S_{11} and axial ratio are maintained along switching between the two states, which is an advantage of this design. This can be observed from Figure 4.14, where S_{11} in state 3 is almost the same as in state 4. Similarly, in Figure 4.15 axial ratio is kept the same in both switching states. The achieved impedance and axial ratio bandwidths calculated from simulation in comparison to measurements are listed in Table 4.2. From Table 4.2, the measured effective bandwidth is 7% (2.4-2.575GHz), which is reasonably wideband for polarization agile microstrip antenna designs.

Antenna radiation pattern at 2.45GHz is shown in Figure 4.17. Good match between simulated and measured results is obtained. The radiation pattern in yz plane remains the same after switching, whereas in xz plane, the radiation pattern is mirrored due to the symmetry of the structure. Experimental results along with the simulated one for the antenna gain versus frequency are shown in Figure 4.18.

Again, because of the symmetry the broadside gain is the same in both modes of the antenna. To avoid redundancy, only RHCP mode is shown. Maximum gain realized is 8.7 dBi at 2.45GHz according to both simulation and measurement, whereas the gain bandwidth is 2.31 - 2.71GHz (16%) from simulation, and 2.31-2.63 GHz (13%) from measurement.

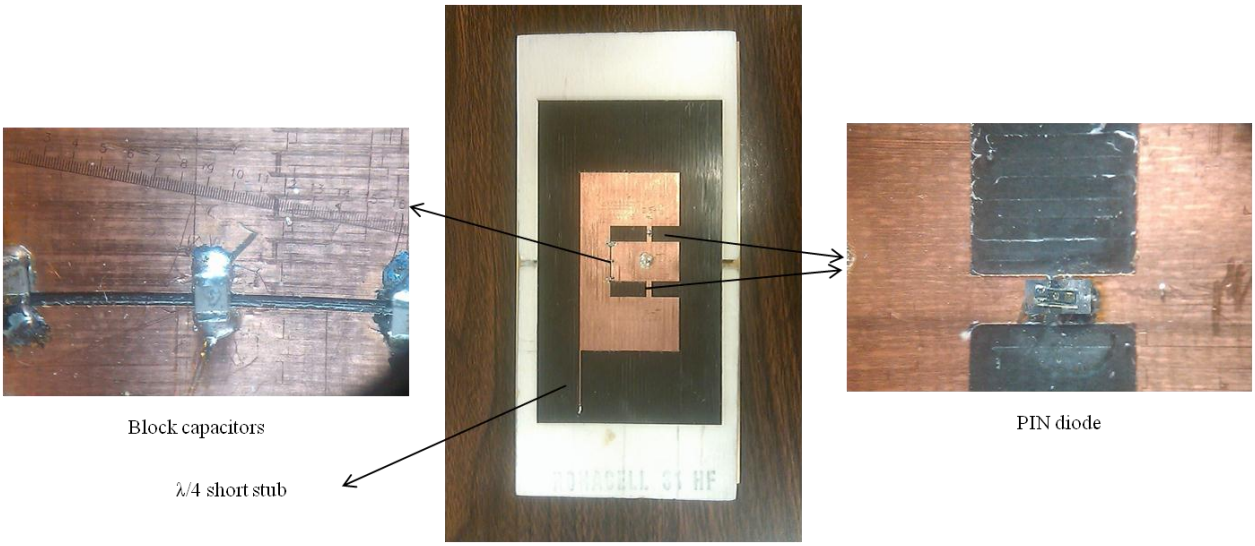

Figure 4.14 Polarization reconfigurable E-shaped patch antenna prototype. Two PIN diodes are used for switching. Metallic pads are printed on each slot to allow the mounting of the diodes. Three block capacitors are mounted across the narrow slit that divides the E-shaped patch. λ/4 transmission line is connected to the corner edge of the patch, whereas from the other side it is connected to a via going to the ground. It acts as a λ/4 short stub, and form high impedance at the edge of the patch to keep RF currents on it unperturbed.

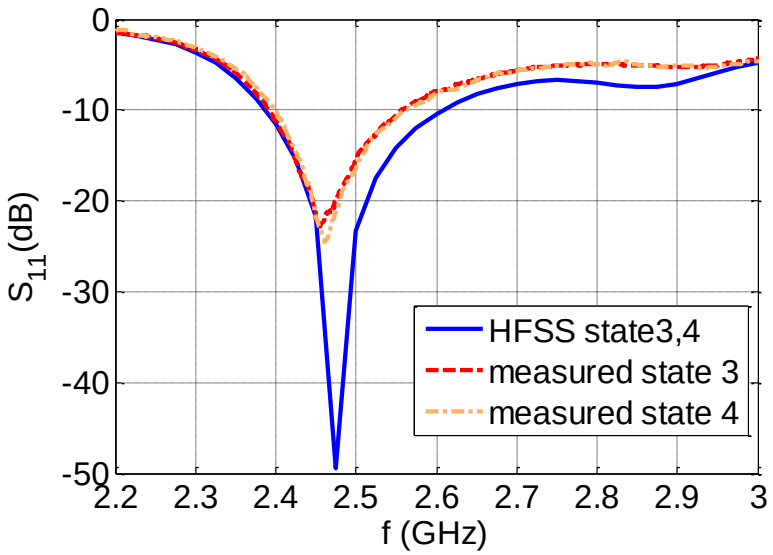

Figure 4.15 Simulated and measured S_{11} for the proposed antenna in states 3, 4.

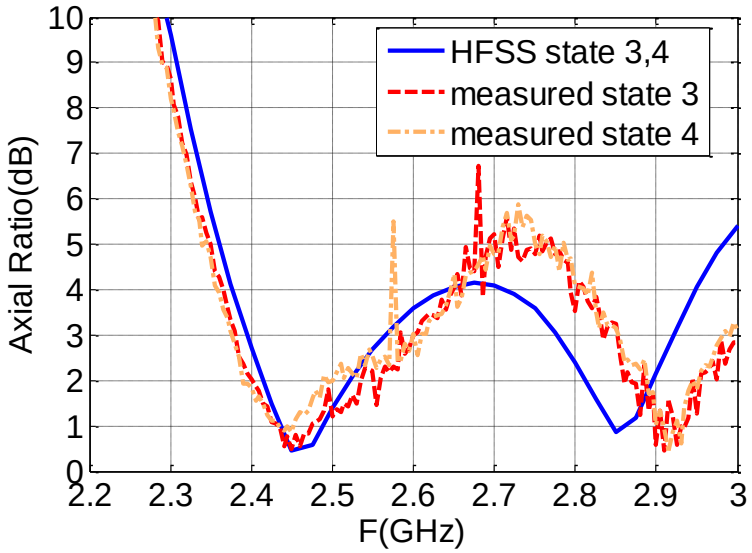

Figure 4.16 Simulated and measured axial ratio for the proposed antenna in states 3, 4.

Table 4.2 Antenna bandwidth simulated vs. measured results at states 3, 4

Quantity	Simulation	Measured
S_{11} (< -10dB)	2.39-2.6 GHz (8.4%)	2.4-2.575 GHz (7%)
Axial ratio (< 3dB)	2.4-2.6 GHz (8%)	2.38-2.6GHz (8.8%)

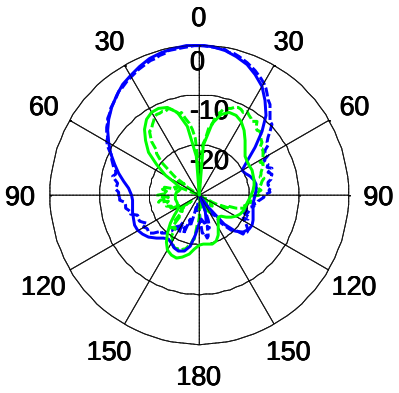

(a)

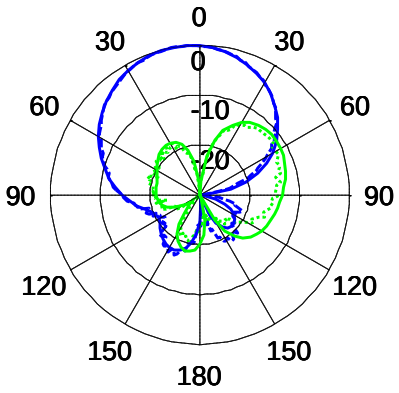

(b)

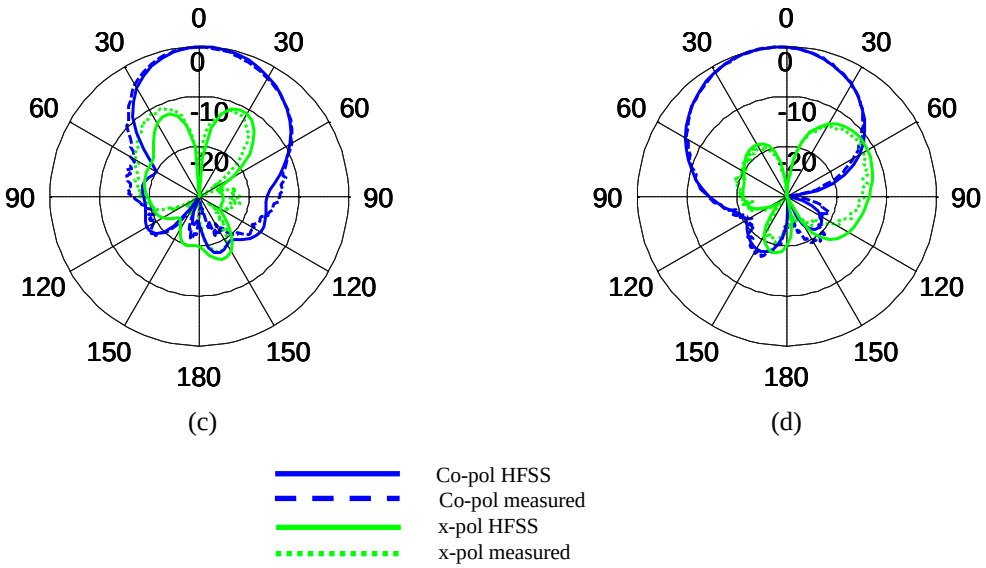

Figure 4.17 Simulated and measured radiation pattern of the proposed antenna. (a) x-z plane at state 3. (b) y-z plane at state 3. (c) x-z plane at state 4 (d) y-z plane at state 4.

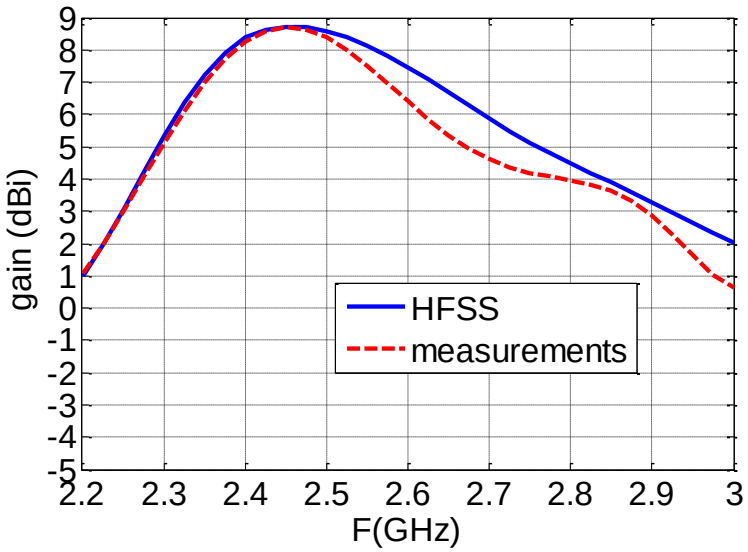

Figure 4.18 Simulate and measure gain of the proposed antenna in either states 3 or state 4.

CHAPTER 5

CONCLUSION AND FUTURE WORK

5.1 Contributions

New technique to achieve circularly polarized radiating fields from single-feed single-layer microstrip antenna using asymmetric E-shaped patch has been proposed. The technique is inherently simple, and achieves wideband axial ratio compared to other techniques applied on comparable size patches. The CP E-shaped patch has been designed, fabricated, and measured for 802.11b/g WLAN band. An effective bandwidth of 9% is obtained (2.34-2.57GHz). Wireless devices that require circular polarization characteristics are considered one of the potential applications for this antenna.

Polarization reconfigurable microstrip antenna has been proposed. The design addresses several drawbacks in the former works that achieve polarization agile antennas. First, simplicity: where it starts with simple E-shaped patch, then optimizing switches position on its slots, with no need for simultaneous optimization of many parameters that yields design complexity. Also, only two switches are used with a simple DC biasing network for integration with the antenna. Second, bandwidth: where wide bandwidth performance is always a challenge for polarization agile microstrip antennas. The 7% effective bandwidth has been realized, and the performance is almost the same going from one state to the other.

Third, antenna gain: some designs shift to slot antenna to achieve polarization reconfigurability with wideband performance. However, the realized gain is smaller compared to the one attained by microstrip patch antennas. The new design realized 8.7dBi maximum gain. For demonstration, the proposed prototype covers the WLAN IEEE 802.11b/g frequency band, making it a candidate for stationary terminals of various wireless communication systems.

5.2 Future Work

Phased array has potentials in numerous applications, like radar and wireless communication systems. Among the major advantages it provides high gain electronically scanned beam. The increasing demand on high-throughput wireless communication drives the introduction of wideband solutions. Most wireless systems use linear polarized phased array antennas. The drawback of this is the sensitivity to the polarization angle. Therefore, further investigation of phased array with wideband polarization agile antenna is aspiring.

BIBLIOGRAPHY

[1] hyperphysics.phy-astr.gsu.edu/hbase/phyopt/quarwv.html

[2] rf-bfioptilas.co.uk/Amotech-163.htm

[3] M A Kossel, R Kung, H. Benedickter, and W. Bachtold, "An Active Tagging System Using Circular Polarization Modulation," *IEEE Trans. Microw. Theory Tech*., vol. 47, no. 12, pp. 2242-2248, Dec. 1999.

[4] P. Y. Qin, Y. J. Guo, and C. H. Liang, "Effect of Antenna Polarization Diversity on MIMO System Capacity," *IEEE Antennas Wireless Propag. Lett*, vol. 9, pp. 1092–1095, 2010.

[5] R. Garg, P. Bhartia, I. Bahl, and A. Ittipiboon, Microstrip Antenna Design Handbook. Boston, London: Artech House, 2001.

[6] C. A. Balanis, Antenna Theory: Analysis and Design. Second edition, John Wiley and Sons, New York, 1997.

[7] http://www.g6lvb.com/images/dualbandpatch001.jpg

[8] www.globalspec.com/FeaturedProducts/Detail/SpectrumAdvancedSpecialtyProducts/New_Dual_Frequency_Patch_Antenna/69411/0

[9] T. Huynh and K. F. Lee, "Single-Layer Single-Patch Wideband Microstrip Antenna," *Electron. Lett.*, vol. 31, no. 16, pp. 1310–1312, Aug. 1995.

[10] K. F. Lee, K. M. Luk, K. F. Tong, Y. L. Yung, and T. Huynh, "Experimental Study of The Rectangular Patch with a U-Shaped Slot," in *Antennas and Propagation Society Int. Symp. AP-S Digest*, July, vol. 1, pp. 10–13, 1996.

[11] K. F. Lee, S. S. Yang, A. Kishk, and K. M. Luk, "The Versatile U-Slot Patch Antenna," *IEEE Antennas Propagat. Mag.*, vol. 52, no. 1, pp. 71-88, February 2010.

[12] K. M. Luk, C. L. Mak, Y. L .Chow, and K. F. Lee, "Broadband microstrip patch antenna," *Electron. Lett.*, vol. 34, no. 15, pp. 1442–1443, 1998.

[13] C. L. Mak, K. M. Luk, and K. F. Lee, "Experimental Study of a Microstrip Patch Antenna with an L-Shaped Probe," *IEEE Trans. Antennas Propag.*, vol. 48, no. 5, pp. 777-783, May 2000.

[14] F. Yang, X. X. Zhang, X. Ye, and Y. Rahmat-Samii, "Wide Band E-Shaped Patch Antenna for Wireless Communications", *IEEE Trans. Antennas Propag.*, vol. 49, no. 7, pp. 1094-1100, July 2001.

[15] W. K. Lo, J. l. Hu, C. H. Chan, and K. M. Luk, "L-Shaped Probe-Feed Circularly Polarized Microstrip Patch Antenna with a Cross Slot," *Microw. Opt. Technol. Lett.*, vol. 25, no. 4, pp. 251-251, May 2000.

[16] F. S. Chang, K. L. Wong, and T. W. Chiou, "Low-Cost Broadband Circularly Polarized Patch Antenna," *IEEE Trans. Antennas Propag.*, vol. 51, no. 10, pp. 2006-2009, October 2003.

[17] K. F. Tong and T. P. Wong, "Circularly Polarized U-Slot Antenna," *IEEE Trans. Antennas Propag.*, vol. 55, no. 8, pp. 2382-2385, August 2007.

[18] S. L. S. Yang, K. F. Lee, and A. A. Kishk, K. M. Luk**,** "Design and Study of Wideband Single Feed Circularly Polarized Microstrip Antennas," *Progress In Electromagnetics Research,* vol. 80, pp. 45–61, 2008.

[19] F. Yang and Y. Rahamt-Samii, "Reconfigurable Patch Antenna Using Switchable Slots for Circular Polarization Diversity," *IEEE Microw. Wireless Compon. Lett.*, vol. 12, no. 3, pp. 96-98, March 2002.

[20] Y. J. Sung, T. U. Jang, and Y. S. Kim, "Reconfigurable Microstrip Antenna with Switchable Polarization," *IEEE Microw. Wireless Compon. Lett.*, vol. 14, no. 11, pp. 534-536, November, 2004.

[21] S. H. Hsu and K. Chang, "A Novel Reconfigurable Microstrip Antenna with Switchable Circular Polarization," *IEEE Antenna and Wireless Propag. Letters,* vol. 6, pp. 160-162, 2007.

[22] Y. J. Sung, "Reconfigurable Patch Antenna for Polarization Diversity," *IEEE Trans. Antennas Propag.,* vol. 56, no. 9, pp. 3053-3054, September, 2008.

[23] Y. F. Wu, C. H. Wu, D. Y. Lai, and F. C. Chen, "A Reconfigurable Quadri-Polarization Diversity Aperture-Coupled Patch Antenna," *IEEE Trans. Antennas Propag.,* vol. 55, pp. 1009–1012, Mar. 2007.

[24] P. Y. Qin, A. R. Weily, Y. J. Guo, and C. H. Liang, "Polarization Reconfigurable U-Slot Patch Antenna," *IEEE Trans. Antennas Propag*., vol. 58, no. 10, pp. 3383-3388, October 2010.

[25] B. Kim, B. Pan, S. Nikolaou, Y. S. Kim, J. Papapolymerou, and M. M. Tentzeris, "A Novel Single-Feed Circular Microstrip Antenna with Reconfigurable Polarization Capability," *IEEE Trans. Antennas Propag.,* vol. 56, no. 3, pp. 630-638, March 2008.

[26] R. H. Chen and J. Row, "Single-Fed Microstrip Patch Antenna with Switchable Polarization," *IEEE Trans. Antennas Propag.,* vol. 56, no. 4, pp. 922-926, April 2008.

[27] K. Chang, I. Bahl, and V. Nair, *RF and Microwave Circuit and Component Design for Wireless Systems*. New York: Wiley-Interscience, 2002.

[28] http://www.skyworksinc.com/Products_Diodes.aspx

[29] E. Brown, "RF-MEMS Switches for Reconfigurable Integrated Circuit," *IEEE Trans. Microwave Theory Tech.*, vol.46, no.11, pp. 1868-1879, November, 1998.

[30] http://www2.laas.fr/laas/images/TEAM/Salle-Blanche/Electrochimie/Electrochimie-savoir-faire/resize1-mEMS-RF_2.jpg

[31] High Frequency Structure Simulation (HFSS), Version 13, Ansoft Corp., Canonsburg, PA, 2010.

[32] A. Khidre, K. F. Lee, F. Yang, and Atef Z. Elsherbeni "Wideband Circularly Polarized E-Shaped Patch Antenna for Wireless Applications," *IEEE, Antennas Propag. Mag.*, vol. 52, no. 5, pp. 219-229, October, 2010.

[33] Data Sheet of 600F100 RF capacitor, ATC, Application Note, www.atceramics.com

[34] American Technical Ceramics Corp., Product Selection Guide, www.atceramics.com/pdf/prod_select%284%29.pdf

[35] Richard Fiore, "Considerations for Optimal Capacitive Coupling," *Microwave Product Digest*, March 2004.

[36] Data Sheet of MA4SPS402 PIN Diodes , MA-Com, Application Note, www.macomtech.com/datasheets/MA4SPS402.pdf

LIST OF PUBLICATIONS

Conference

[1] Ahmed Khidre, Kai-Fong Lee, Atef Z. Elsherbeni, and Fan Yang, "Circularly Polarized E-Shaped Patch Antenna for Wireless Communications," in *UCNC-URSI Radio Science Meeting Digest*, July 2010.

[2] Ahmed Khidre, Kai-Fong Lee, Atef Z. Elsherbeni, and Fan Yang, "E-shaped Patch Antenna with Reconfigurable Circular Polarization for Wireless Applications," in *ACES Int. Rev. of Progress in Applied Comp. Electromag., Digest*, pp. 822-826, July 2010.

Journals

[3] Ahmed Khidre, Kai-Fong Lee, Fan Yang, and Atef Z. Elsherbeni, "Wide Band Circularly Polarized E-Shaped Patch Antenna for Wireless Applications," *IEEE, Ant. Propap., Mag.,* vol. 52, no. 5, pp. 219-229, October, 2010.

[4] Ahmed Khidre, Kai-Fong Lee, Fan Yang, and Atef Z. Elsherbeni, "Wide Band Circularly Polarized E-Shaped Patch Antenna for Wireless Applications," (in revision for *IEEE Trans. Ant. Propag.*)

VITA

Ahmed Khidre received his B.Sc in electrical engineering from Ain Shams Uiversity in 2006. From 2006 to 2007, he was employed at Ericsson Egypt Ltd. From 2007 to 2009, he was appointed as a teacher assistant at the electrical engineering department of Misr International University (MIU). He has joined The University of Mississippi since 2009, as a research asssitant and gradute student in the center of appplied electromagnetic systems research (CEASR). Currently, he is working toward his PhD degree. Khidre, is a technical reviewer for "*IEEE Transaction on Antennas and Propagation"*, as well as "*Progress in Electromagnetic Research"* refreed journals. His research interest includes the analysis, desing, and measuments of printed antennas, reconfigurable antennas and tunable microwave circuits, beam scanning antennas, UWB communication systems, FDTD for EM modeling and simulation, and nanotechnology for electromagnetics (RF MEMs, Carbon nanotubes, micromachining).